

Report

On

**MODELING THE EFFECTIVE COMPOSITE PROPERTIES OF FIBER
REINFORCED POLYMERS WITH NANO INCLUSIONS**

Submitted in partial fulfillment of the requirements of the course

Practice School II

By

PENDYALA ABHIJEET

2009A4PS343H

At



NATIONAL AEROSPACE LABORATORIES, BANGALORE

Under the guidance of

Dr. S. Raja

Senior Principal Scientist & Group Head

Dynamics and adaptive structures

STTD, CSIR-NAL



Birla Institute of Technology and Science, Pilani

Hyderabad Campus

05-12-2012

BIRLA INSTITUE OF TECHNOLOGY & SCIENCE

PILANI (RAJASTHAN), Hyderabad Campus

Practice School Division

Station	:	National Aerospace laboratories
Centre	:	Bangalore
Duration	:	5 ½ months
Date of Commencement	:	4 th July, 2012
Date of Submission	:	05 ^h December, 2012
Title of the Project	:	MODELING THE EFFECTIVE COMPOSITE PROPERTIES OF FIBER REINFORCED POLYMERS WITH NANO INCLUSIONS
Name of the Student	:	Pendyala Abhijeet
ID No.	:	2009A4PS343H
Discipline of the student	:	B.E. (Hons.) Mechanical
Name of Guide	:	Senior Principal Scientist & Group Head Dynamics and adaptive structures STTD, CSIR-NAL
Name of PS Faculty	:	Dr. Rakesh Mohan Jha, Scientist G, ALD
Project area	:	Effective mechanical properties of fiber reinforced polymers with Nano inclusions.



Signature of Student

Date: 05-12-12

Signature of PS Faculty

Date:

Declaration

I hereby declare that the entire work embodied in the dissertation had been carried out by me and no part of it has been submitted for any degree or diploma of any institution previously.

Place: Bangalore

Date: 05-12-12



Signature of student

(Pendyala Abhijeet)

**BIRLA INSTITUTE OF TECHNOLOGY AND SCIENCE
PILANI (RAJASTHAN)**

PRACTICE SCHOOL DIVISION

Response Option Sheet

Station: National Aerospace Laboratories

Centre: Bangalore

Name: Pendyala Abhijeet

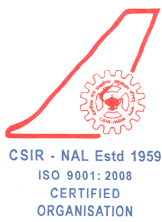
ID Number: 2009A4PS343H

Title of the Project: Modeling the Effective Composite properties of Fiber Reinforced polymers
with Nano Inclusions

Code No.	Response Option	Response (YES/NO)
1	A new course can be designed out of this project	NO
2	The project can help modification of the course content of some existing courses	NO
3	The project can be hosted directly in some existing CDCs/ DCOCs/ EA courses	NO
4	The project can be used in the preparatory courses like AAOC/ ES/TA and core courses	NO
5	The project cannot come under any of the above mentioned options as it relates to the professional work of the host organization	YES

Signature of Student

Signature of PS Faculty



वैज्ञानिक तथा औद्योगिक अनुसंधान परिषद्
राष्ट्रीय वांतरिक्ष प्रयोगशालाएं
Council of Scientific & Industrial Research
National Aerospace Laboratories
पी बी सं / PB No.1779, एचएल एयरपोर्ट रोड / HAL Airport Road, बैंगलुरु / Bangalore- 560 017, भारत / INDIA
फोन / Phone: (का / Off): +91 - 80 - 2527 3351 - 54, 2508 6000 - 6599, फैक्स / Fax : +91 - 80 - 2526 0862, 2527 0670
वेबसाइट / Website : <http://www.nal.res.in>

CERTIFICATE

This is to certify that the project entitled, "**Modeling the Effective composite properties of Fiber Reinforced polymers with Nano inclusions**", submitted by **Mr. Pendyala Abhijeet** in partial fulfilment of the course BITS C412, Practice School II, BITS Pilani is a bonafide record of the work carried out by him at the Structural Technologies Division (STTD), *Council of Scientific and Industrial Research – National Aerospace Laboratories (CSIR-NAL)*, Bangalore from 4th July, 2012 to 14th December, 2012 under my guidance and supervision.

Signature of the guide

Dr. S. Raja

Senior Principle Scientist & Group head

Dynamics and adaptive structures

STTD, CSIR-NAL

Bangalore.

ACKNOWLEDGEMENT

I would like to express my thanks to **Dr. Shyam Chetty**, Acting Director, NAL and **Dr. J.S Mathur**, Head KTMD, NAL for giving me an opportunity to carry out my project work at NAL.

I am also grateful to **Dr. B.N.Jain**, Director and Vice Chancellor, BITS Pilani and **Dr. G Sundar**, Dean, Practice School II for allowing me to do my PS II in such a reputed organization.

I would like to thank **Dr.S. Raja**, Senior Principal Scientist & Group Head Dynamics and adaptive structures for letting me use the Aeroelasticity and smart structures lab.

I would like to thank my PS instructor **Dr. Rakesh Mohan Jha**, Scientist G, CEM for his guidance and allotment of projects.

I would also like to express my thanks to **Mr. Abhinav Alva**, **Mr. Dwarakanathan** **Mr.Karthikeyan**, **Mr. Veda Prakash** and all STTD staff for their support and for helping me to carry out the project to the best of my abilities.

List of Figures

- Fig. 1 Carbon Nanotube
- Fig. 2 Flow chart representing Modeling Methods and Tools
- Fig. 3 Flow chart representing Various Material Modeling Techniques
- Fig. 4 Representative Volume element in Method of Cells
- Fig. 5 Schematic of nano-CFRP Hybrid Composite
- Fig. 6 Flow chart representing Multistep Homogenization Scheme
- Fig. 7 CFRP composites with CNTs aligned in longitudinal direction
- Fig. 8 Variation of Elastic constants at wt% = 2.0 & Aspect Ratio = 1000 with Volume fraction of CFRP
- Fig. 9 CFRP composites with CNTs aligned in transverse direction
- Fig. 10 Variation of Elastic constants at wt% = 2.0 & Aspect Ratio = 1000 with volume fraction Of CFRP
- Fig. 11 CFRP composites with randomly oriented CNTs
- Fig. 12 Variation of Elastic constants at wt% = 2.0 & Aspect Ratio = 1000 with volume fraction Of CFRP
- Fig. 13 Schematic of Laminate
- Fig. 14 2-d lamina under axial load and bending moments
- Fig. 15 Variation of stress and strain in a laminate with respect to distance from midplane
- Fig. 16 Convention for height of laminate from midplane
- Fig. 17 nano-CFRP hybrid Composite case 111-Ort1
- Fig. 18 nano-CFRP hybrid Composite case 222-Ort1
- Fig. 19 nano-CFRP hybrid Composite case 222-Ort2
- Fig. 20 Portion of a laminate subjected to a shear force, P, and the resulting normal stress distribution on an arbitrary cross section
- Fig. 21 original (actual) and transformed laminate cross-sections.
- Fig. 22 section of laminate acted upon by the horizontal shear force, H, and the distributed normal stress
- Fig. 23 Distribution of ILSS with thickness : Brett A. Bednarcyk et al
- Fig. 24 Distribution of ILSS with thickness modeled in Matlab
- Fig. 25 Distribution of ILSS with thickness : Brett A. Bednarcyk et al
- Fig. 26 Distribution of ILSS with thickness modeled in Matlab
- Fig. 27 T_{yz} Distribution of 0-0-0 [cfrp nano-cfrp cfrp]
- Fig. 28 T_{yz} Distribution of 0-45-0 [cfrp nano-cfrp cfrp]
- Fig. 29 T_{yz} Distribution of 0-90-0 [cfrp nano-cfrp cfrp]
- Fig. 30 T_{yz} Distribution of 45-0-45 [cfrp nano-cfrp cfrp]
- Fig. 31 T_{yz} Distribution of 0-0-0[nano-cfrp cfrp nano-cfrp]
- Fig. 32 T_{yz} Distribution of 0-45-0 [nano-cfrp cfrp nano-cfrp]
- Fig. 33 T_{yz} Distribution of 0-45-0 [nano-cfrp nano-cfrp nano-cfrp]

List of Tables

- Table. 1 Validation of Epoxy/CNT/Carbon Fiber System
- Table. 2 Validation of Epoxy/CNT/Carbon Fiber System
- Table. 3 Validation of Epoxy/CNT System
- Table. 4 Validation of Epoxy/ Carbon Fiber System
- Table. 5 Layer wise Maximum ILSS- T_{yz} values before and after nano inclusion of [cfrp,nano-cfrp,cfrp] system with 1% of cnt.
- Table. 6 Layer wise Maximum ILSS- T_{yz} values before and after nano inclusion of [nano-cfrp,cfrp,nano-cfrp,] system with 1% of cnt..
- Table. 7 Layer wise Maximum ILSS- T_{yz} values before and after nano inclusion of [nano-cfrp,nano-cfrp, nano-cfrp] system with 1% of cnt.
- Table. 8 Layer wise Maximum ILSS- T_{yz} values before and after nano inclusion of [cfrp,nano-cfrp,cfrp] system with 2% of cnt.
- Table. 9 Layer wise Maximum ILSS- T_{yz} values before and after nano inclusion of [nano-cfrp ,cfrp,nano-cfrp] system with 2% of cnt.
- Table. 10 Layer wise Maximum ILSS- T_{yz} values before and after nano inclusion of [nano-cfrp , nano-cfrp,nano-cfrp] system with 2% of cnt.

Contents

AIM	x
SCOPE	x
ABSTRACT	xi
CHAPTER-1: Introduction	1
CHAPTER-2: Literature review	
2.1 Introduction	3
2.2 Modeling effective moduli using micromechanics	6
2.3 Micromechanics models.....	7
2.4 Method of cells.....	8
2.5 nano-CFRP hybrid composite	10
2.6 Interlaminar Shear stress	14
CHAPTER-3: nano-CFRP hybrid composite	
3.1 Introduction	15
3.2 Multiscale Constitutive modeling	16
CHAPTER-4: Validations of Multiscale Constitutive model	18
CHAPTER-5: Simulations of nano-CFRP hybrid composite lamina	
5.1 Simulations of nano-CFRP	22
5.2 Observations.....	25
CHAPTER-6: Composite Laminate	
6.1 Introduction	26
6.2 Laminate Theory	27
6.3 simulations of nano-CFRP hybrid composite laminate	30
CHAPTER-7: Interlaminar Shear Stress [ILSS]	
7.1 Introduction	34
7.2 Modeling ILSS: Simplified Shear Model	35
7.3 Validations of ILSS	39
7.4 Damage Tolerant laminates with Cnt inclusions	41
7.5 Simulations.....	41
7.6 Conclusions	49
Conclusions	50
References	51

AIM

New structural concepts, particularly polymer-based nanocomposites, have been pursued in recent years to harness the attractive properties of carbon nanotubes (CNTs). In this work micromechanics modeling of hybrid advanced composite materials are described and characterized which exhibits enhanced multifunctional laminate-level engineering properties. The hybrid system is comprised of three parts: Carbon fibers (dia. of order microns), a thermoset polymer resin, and CNTs (dia. of order nanometers) organized within the polymeric matrix. The project aims to develop a constitutive model to predict the composite properties of Hybrid composite system such as carbon fiber polymers reinforced with different kind of inclusions such as short fibers, particulates and cylindrical nano-reinforcements such as carbon nanotubes. The project also focuses on prediction of Effective mechanical properties and interlaminar shear stresses for a hybrid composite laminate.

SCOPE

Carbon-fiber based advanced composites form the majority of advanced composites used in aerospace, automobile and other high-performance applications. A promising structural application for CNTs is reinforcement of traditional fiber-reinforced plastic (FRP) advanced composites. The astonishing mechanical properties of Multiwall Carbon Nanotubes such as high elastic modulus of the order of 1.2 TPa, low density of around 2000 kg/m^3 , high tensile strength of around 150 GPa, unusually high aspect ratio of up to 50000 and its peculiar hollow tubular molecular structure provides a wide scope to be used as reinforcements in polymeric composites. The use of such extraordinary materials as reinforcements in low weight percentages in polymeric matrix systems could be an inexpensive yet effective technique to achieve some exceptional mechanical properties in a composite system. Thus a constitutive model, which will predict the composite properties of such advanced materials, will be very useful in designing such advanced structures.

ABSTRACT

Micromechanics modeling schemes have been extensively used to model the effective moduli of Carbon Nanotubes based composites. In the current work, a micromechanics based multistep homogenization method is used to compute the effective moduli of carbon nanotube reinforced carbon fiber composites. The composite is assumed to be reinforced with two kinds of Carbon Nanotube fibers; namely isolated individual fibers and agglomerated or clustered fibers. A new uniform agglomeration model is introduced which assumes that the size of the carbon nanotube clusters throughout the matrix remains same. Agglomeration volume fraction a critical parameter in the simulation is assumed to be an explicit function of inter-particle distance and quality of dispersion of fibers. The micromechanics model also incorporates random fiber orientation using a statistical approach. It is also shown that these also reduce the stiffening effect of carbon nanotubes significantly. The current model is validated with literature and it has been shown that with incorporation of particle agglomeration and random fiber orientation, it closely predicts the elastic modulus of the nano-CFRP hybrid composite.

Also the effective mechanical properties of a Laminate system were predicted using Laminate theory. In addition to above the project focused on calculating the interlaminar shear stresses in laminates using a Simplified shear model and results were validated with literature. A Novel method is introduced to enhance the interlaminar shear stress without modifying the laminate parameters like thickness, number of layers and orientation of plies.

Chapter-1

INTRODUCTION

One of the hallmarks of carbon research over the last decade is the discovery of fullerenes and carbon nanotubes (CNTs)[1]. CNTs have attracted a lot attention due to their unique structural properties, remarkable physical properties and their versatile applications, such as field-emission displays, Nano composite materials, tissue scaffolds, energy storage/conversion systems, probes, Nano sensors and Nano devices [2]. CNTs can be visualized as graphitic sheets rolled into seamless long cylinders, as shown in Figure They have diameters ranging from 0.6nm to 100nm [3], while the lengths range from several hundred nanometers to several micrometers. The intriguing structures have evoked much interest and a large amount of research has been dedicated to their understanding. The most common types of CNTs include Single-Wall Carbon Nanotubes (SWNTs) and Multi-Wall Carbon Nanotubes (MWNTs). SWNTs have a wall that is one atom thick with diameters in the range of 0.6-1.4nm [3]. MWNTs can be regarded as a coaxial assembly of multiple walls with diameters in the range of 1.4-100nm [4].

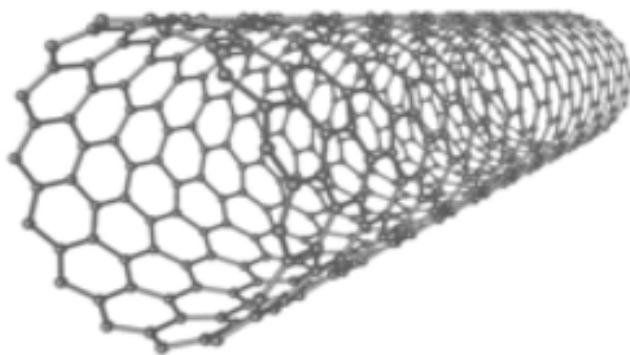


Fig.1 Carbon Nanotube

In addition to their unique sizes and shapes, CNTs attracted attention also because of their remarkable physical properties, including: (1) exceptional electrical conductivity and current carrying capacity: CNTs exhibit the characteristics of a metal or a semiconductor depending on its chirality [5]; (2) excellent thermal conductivity: the thermal conductivity of SWNT is about 1750-5800W/mK, which makes SWNTs the best heat-conducting material we have ever known [6]; (3) super mechanical strength: the tensile strength of SWNTs is about 50-200GPa, the Young's modulus is about 1TPa and the failure strain is about 20-30%

[7].

Compared with conventional reinforcing fillers, the incorporation of Nano scale constituents into composites leads to more significant enhancements of material properties. In Nano composites, the reinforcing phase has at least one dimension less than 100 nm, which may overcome the common micro-scale defects in parts. The advantages of Nano composites include better electrical and thermal conductivity, improved strength and modulus, lower coefficient of thermal expansion, ameliorative flame retardance and enhanced optical clarity, etc.

When fabrics are introduced into CNT based nanocomposites, reinforcing phase includes both conventional fiber and CNT filler. A synergistic combination of conventional fiber, CNT filler and polymer results in a multiscale composite, which has a hierarchical structure ranging from nanoscale CNTs to micron size fibers. Because of the exceptional structural and physical properties of CNTs, CNT additives are very promising to enhance the through-thickness properties by fastening the adjacent fabric layers in 3D composites.

It is also highly desired that the addition of CNTs will result in significant enhancement of thermal, electrical and mechanical properties of polymer matrix at relatively small concentrations. Therefore, CNT based multiscale composites will demonstrate structural [8-14] and multi-functional capabilities simultaneously, such as damping resistance [15], actuation [16-19] and sensing [20-22] capabilities.

All of these remarkable properties make CNTs one of the most promising reinforcements in advanced polymeric composites applications, and also evoke great interest in a better understanding of CNTs/polymer flow behavior during composite manufacturing. However, the extent to which the mechanical properties can be improved depends on several factors like uniformity of dispersion, degree of alignment of CNT's, and the strength of CNT/polymer interfacial bonding. Since it is difficult to control and measure simultaneously many of these parameters experimentally, computational modeling can provide some crucial insights and will help to establish the behavioral aspects of nanocomposites.

Chapter-2

LITERATURE REVIEW

2.1 Introduction

Experimental based research can ideally be used to determine structure-property relationships of nanostructured composites, experimental synthesis and characterization of nanostructured composites demands the use of sophisticated processing methods and testing equipment; which could result in exorbitant costs. To this end, computational modeling techniques for the determination of mechanical properties of nanocomposites have proven to be very effective [23-30]. Computational modeling of polymer nanocomposite mechanical properties renders the flexibility of efficient parametric study of nanocomposites to facilitate the design and development of nanocomposite structures for engineering applications.

Mechanical properties of nanostructured materials can be determined by a select set of computational methods. These modeling methods span a wide range of length and time scales, as shown in Fig. 2. For the smallest length and time scales, Computational Chemistry techniques are primarily used to predict atomic structure using first-principles theory. For the largest length and time scales, Computational Mechanics is used to predict the mechanical behavior of materials and engineering structures. Computational Chemistry and Computational Mechanics modeling methods are based on thoroughly-established principles that have been developed in science and engineering. However, the intermediate length and time scales do not have general modeling methods that are as well developed as those on the smallest and largest time and length scales. Therefore, Multiscale modeling techniques are employed, which take advantage of Computational Chemistry and Computational Mechanics methods simultaneously for the prediction of the structure and properties of materials.

Figure-3 is a schematic that details the relationship of specific modeling techniques in Computational Mechanics and Computational Chemistry. The continuum-based methods primarily include techniques such as the Finite Element Method (FEM), the Boundary Element Method (BEM), and the micromechanics approach developed for composite materials. Specific Micromechanical techniques include Eshelby approach, Mori-Tanaka method, Halpin-Tsai method, Method of cells [31-41]. The molecular modeling tools include molecular dynamics, Monte Carlo, and Ab-initio techniques.

Modeling Methods

Computational Chemistry

Multiscale Modeling

Computational Mechanics

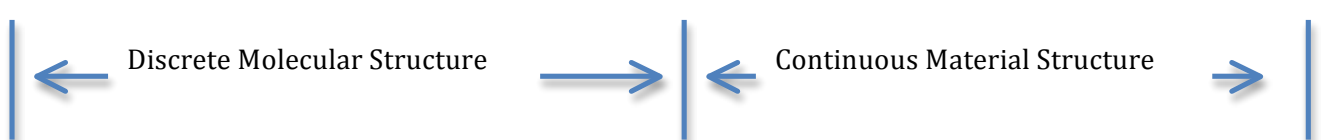
Modeling tools

Quantum mechanics

Nanomechanics

Micromechanics

Structural mechanics



Length Scale



Time Scale



Fig. 2
Flow chart representing Modeling Methods and Tools

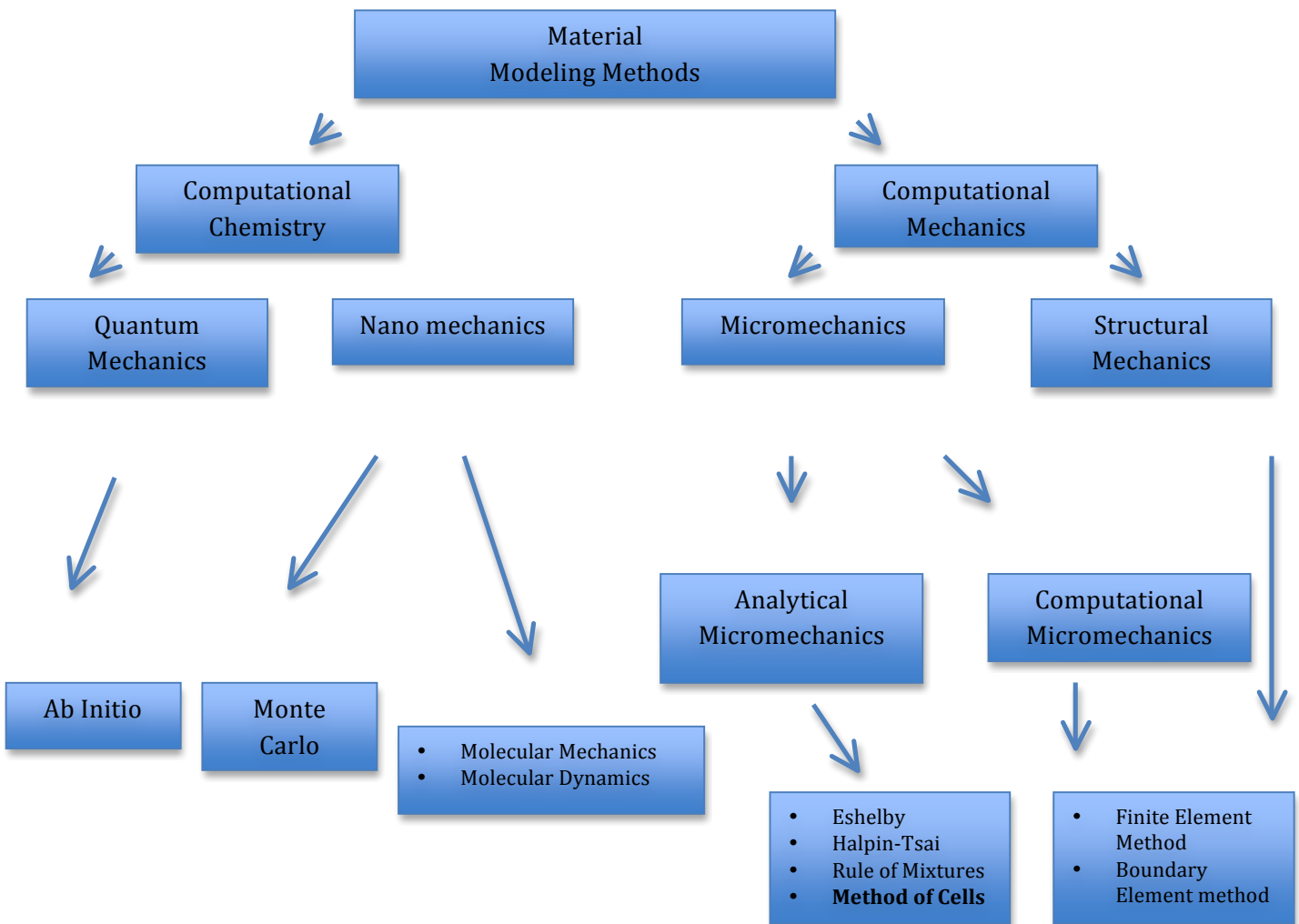


Fig. 3
Flow chart representing Various Material Modeling Techniques

2.2 Modeling the effective moduli of Nanocomposites using Micromechanics

- Nano reinforcements have very high aspect ratio, high specific surface area, very large particles/ unit volume which makes them very superior compared to any other kind of reinforcements. [2-3]
- When the reinforcement size is very large it is bound to have
 - Disorders due to dislocations, defects and voids
- As the particle scale is reduced to nano dimension, the overall material defects also tend to reduce and therefore, nano reinforcements are almost defect free.
- It is known fact that when the length of the fiber is of the order of 25-100 μm (E.g. CNTs), good load transfer occurs as in the case of any other reinforcements.
- Thus, Micromechanics based modeling schemes have been extensively used to characterize the effective material properties of nanocomposites.
- Micromechanics based modeling assumes perfect load transfer between reinforcement and resin and does not consider the following effects:
 - Chemical bonding
 - Intra molecular forces
 - Particle statics and dynamics
 - Thermodynamic energy at molecular level
- For reinforcements like CNT's which have their length scale in microns and diameter in nanometers, micromechanics could still be applied to evaluate the material properties of their composites.
- Due to fabrication limitations, it is difficult to orient the fibers in a required direction, and thus random orientation of fibers reduces the stiffening effect considerably.

- Due to very narrow separation between nanofibers (such as CNTs), Van Der Waals forces result in particle agglomerations, which also reduce their stiffening effect.
- Hence while modeling these effects; it is necessary that the representative volume element is assumed to be periodic.
- All micromechanics based modeling schemes considers the volume fraction of reinforcement and matrix for evaluating the composite properties, therefore the effect of change in dimension from micro to nano scale is not considered.
- When the nano reinforcements are randomly oriented in the matrix, the composite properties are similar to that of an isotropic material else when they are aligned in a specified direction, it behaves like a transversely isotropic material.

2.3 Micromechanics models

Many micromechanics based modeling techniques have been used to model the effective material properties of Nanocomposites. Some of the popular ones are:

1. Voigt model/Piggot formulations (modified rule of mixtures)[42]
 - Voigt model is based directly on rule of mixtures
 - Piggot formulations is modified rule of mixtures using a proper scaling factor to take random fiber orientations into account
 - Applicable only at very low weight percentages
2. Shear Lag model[43,44]
 - Shear lag model considers fiber dimensions in rule of mixtures
 - The representative volume element considers fiber placed in a concentric cell
 - Applicable only at very low weight percentages
3. Halpin Tsai model[45-49]
 - Halpin Tsai model is a derivative from rule of mixtures

- Random fiber orientation factor is considered in an efficient manner
 - Fiber agglomerations are also considered using a variable shape factor
 - It's a semi-empirical approach
 - Requires additional inputs and curve fitting techniques for simulations
 - Applicable even at higher weight percentages

4. Mori-Tanaka model[50]

- Similar to Halpin tsai model

2.4 Method of Cells

Method of Cells (MOC) has been originally developed for long fiber systems and aligned short fibers[51]. It's a micromechanics based model, which considers matrix, fiber properties and fiber dimensions.

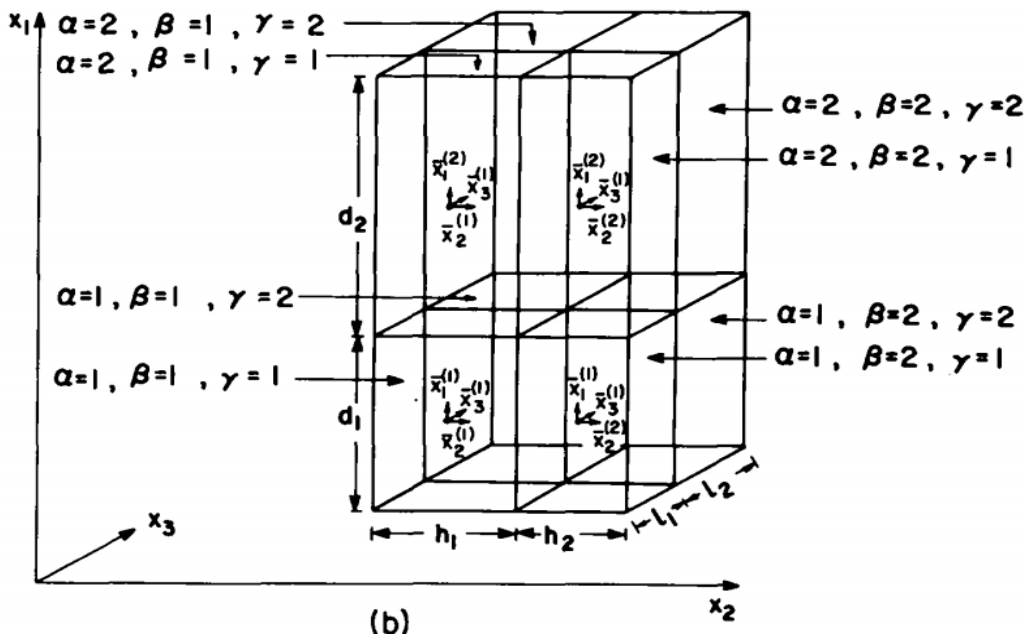


Fig.4 Representative Volume element in Method of Cells

The MOC has been successfully used to model:

- Infinite long fiber-matrix composites

- Bilaminates
- Particulates
- Aligned finite short fiber-matrix composites

To model nanocomposites, 3 essential parameters are further considered in MOC[52]. They are:

- Equivalent volume of fiber
- Random orientation of fiber in the matrix
 - Random orientation has been incorporated using a statistical averaging approach by considering finite number of fibers
- Agglomeration of fibers in the matrix
 - A uniform agglomeration model is considered by assuming a constant cluster size throughout the matrix
 - Composite is assumed to be consisting of two reinforcements; isolated and agglomerated fiber
 - Equivalent composite property is evaluated using a multistep homogenization model.

Inferences:

- Method of cells (2D & 3D) can effectively be used for long fiber as well as short fiber reinforcements in various types of matrix systems respectively, by solving and finding all the closed form constitutive relations
- To model nanocomposites, it is necessary to introduce parameters which will simulate the random orientation and homogenization of nano particles in the matrix.

2.5 nano-CFRP Hybrid Composites

The preparation of nano-CFRP hybrid composites and blends is mainly for five aims:

(1) To prevent inter fiber-fracture

The cohesive matrix fracture and adhesive fracture of the fiber/matrix interface are known as inter-fiber fracture. The inter-fiber fracture is macro-damage that starts by the initiation of matrix micro-cracks at the fiber/matrix interface during matrix curing or due to transverse stress as a result of (off-axis) loading, thermal stresses, or fatigue loading. The micro-cracks subsequently propagate through the matrix to form macro-cracks. The macro-cracks would lead to full fracture in the case of one-layer composite plate and severe damage in the case of multi-layered composite laminate. The inter-fiber fracture is therefore known to govern shear strength of FRPs. This aspect becomes very important in FRP pultruded sections where shear strength is a typical design limitation when extreme loading such as impact, blast, or seismic is of interest.

(2) To overcome premature failure due to low mechanical properties in the transverse direction to the fiber constitutes which is a fundamental weakness of fiber reinforced polymeric composites.

(3) The low failure strain and ductility are other drawbacks in the mechanical response when FRPs are loaded in fiber direction (on-axis loading). The relatively low failure strain of FRPs is explained by their lack of plasticity, which is attributed to the relatively low shear strength of the FRP materials (about 5% of its ultimate tensile strength governed by the limited shear strength of the polymer matrix) leading to the absence of yield-like behavior

(4) To enhance the damping efficiency

(5) To overcome failure modes of FRPs like matrix fracture, interlaminar delamination, and fiber-matrix interface debonding.

Eslam Soliman et al [53]

This investigation experimentally examined the role of multi-walled carbon nanotubes (MWCNTs) on the tension (on- axis tension test) and in-plane shear (off-axis tension test) behaviors of carbon fiber reinforced polymer composites. Both pristine and chemically

functionalized MWCNTs were utilized with four different loadings: 0.1, 0.5, 1.0, and 1.5 wt% of epoxy. Their investigation showed that with 1.5 wt% functionalized MWCNTs, failure strain, ultimate strength, and toughness of the off-axis tension test are improved by 39%, 51%, and 121%, respectively. On the contrary, limited improvements were observed for the on-axis tested samples with functionalized or pristine MWCNTs.

Inference:

- 1.) Significant improvements in the mechanical properties were observed in the off-axis tensile behavior of FRP incorporating functionalized MWCNTs. However, no significant effect of the MWCNTs was observed when the composite coupons were loaded on-axis.
- 2.) The pristine MWCNTs were shown to enhance the failure strain only while the functionalized MWCNTs were shown to enhance both the ultimate shear strength and failure strain.

Myungsoo Kim et al [54]

Carbon fiber-reinforced epoxy composites modified with carbon nanotubes (CNTs) were fabricated and characterized. High-energy sonication was used to disperse CNTs in the resin, followed by infiltration of fiber preform with the resin/CNT mixture. The effects of sonication time on the mechanical properties of “multiscale” composites, which contain reinforcements at varying scales, were studied. A low CNT loading of 0.3 wt% in resin had little influence on tensile properties, while it improved the flexural modulus, strength, and percent strain to break by 11.6%, 18.0%, and 11.4%, respectively, as compared to the control carbon fiber/epoxy composite. While sonication is an effective method to disperse CNTs in a resin, duration, intensity, and temperature need to be controlled to prevent damages imposed on CNTs and premature resin curing. A combination of Halpin–Tsai equations and woven fiber micromechanics was used in hierarchy to predict the mechanical properties of multiscale composites, and the discrepancies between the predicted and experimental values were explained.

Inference:

- 1.) A small loading of CNTs (0.3 wt%) had little influence on the fiber-dominated

tensile properties, while it enhanced the matrix-dominated flexural properties significantly. It was demonstrated that CNTs can serve as an efficient filler material that can reinforce the matrix at a small loading.

- 2.) Optimizing the sonication process will help maximize CNT dispersion while minimizing damages imposed on the CNT and preventing premature curing. However, pretreating the fiber or chemically functionalizing the CNTs may be necessary to enhance the interfacial strength

Mandar Kulkarni et al [55]

Premature failure due to low mechanical properties in the transverse direction to the fiber constitutes a fundamental weakness of fiber reinforced polymeric composites. A solution to this problem is being addressed through the creation of nanoreinforced laminated composites where carbon nanotubes were grown on the surface of fiber filaments to improve the matrix-dominated composite properties. The carbon nanotubes increased the effective diameter of the fiber and provide a larger interface area for the polymeric matrix to wet the fiber. A study was conducted to numerically predict the elastic properties of the nanoreinforced composites. A multiscale modeling approach and the Finite Element Method were used to evaluate the effective mechanical properties of the nanoreinforced laminated composite. The cohesive zone approach was used to model the interface between the nanotubes and the polymer matrix. The elastic properties of the nanoreinforced laminated composites including the elastic moduli, the shear modulus, and the Poisson's ratios were predicted and correlated with iso-strain and iso-stress models. An experimental program was also conducted to determine the elastic moduli of the nanoreinforced laminated composite and correlate them with the numerical values.

Inference:

- 1.) It was determined that multiscale modeling can be effectively and conveniently used to study nanoreinforced laminated composites
- 2.) Incorporation of the cohesive zone model in the finite element model captures the interfacial behavior adequately and provides more accurate results than perfect bonding models.

3.) It was shown that the elastic modulus of the NRLC in the transverse direction to the fiber increases several fold respect to the value of the polymer matrix with the addition of about 10% CNT volume content. The results of this study also indicate that the elastic modulus in the transverse direction to the fiber can be better predicted than the elastic modulus in the fiber direction and the Poisson's ratios.

Mao Sheng Chang et al [56]

The synergetic effect of multi-walled carbon nanotubes (MWCNTs), carbon fiber (CF), and glass fiber (GF) on the static and dynamic mechanical and thermal properties of MWCNTs/epoxy (EP), carbon fiber reinforced polymer (CFRP), and glass fiber reinforced polymer (GFRP)/EP composites were studied. Impact, tensile, and flexural strengths and fatigue cycles of MWCNTs/EP, MWCNTs/CFRP/EP, MWCNTs/GFRP/EP were increased with an increase of MWCNTs content in the epoxy resins. The impact strength of MWCNTs/EP composite is increased dramatically from 4.8 J/M (neat resin) to 12.2 J/M (increased 154.1%) by adding 2.0 phr MWCNTs in the composites. The tensile strength of MWCNTs/CFRP/EP was enhanced from 580.1 MPa (CFRP/EP) to 781.4 MPa (increased 34.7%) by adding 0.5 phr MWCNTs. In addition, the flexural strength of MWCNTs/GFRP/EP was increased from 244.1 MPa (GFRP/EP) to 298.1 MPa (increased 22.16%) by adding 0.75 phr MWCNTs. The fatigue cycles of MWCNTs/GFRP/EP were increased from 959 cycles (GFRP/EP) to 3232 cycles (increased 237%) by adding 2.0 phr MWCNTs. The coefficient of thermal expansion (CTE) of MWCNTs/CFRP/EP was decreased significantly by adding 2.0phr MWCNTs. The CTE of GFRP/EP had a value of 65.5ppm/ \square C by adding 2.0 phr MWCNTs and was lower than that of CFRP/EP.

Inference:

- 1.) The enhancement of MWCNTs/GFRP/EP with addition of MWCNTs increased the flexural strength, and was higher than that of MWCNTs/CFRP/EP.
- 2.) The impact strength of GFRP/EP with addition of MWCNTs was improved, higher than that of MWCNTs/ CFRP/EP.
- 3.) The fatigue cycles of MWCNTs/ GFRP/EP by adding MWCNTs was cycles higher than that of MWCNTs/CFRP/EP.

2.6 Interlaminar shear stress

R. Rolfs et al [57]

A simple method of improving the transverse shear stress results within finite element calculations based on the First Order Shear Deformation Theory has been demonstrated. The basic idea consists in directly calculating the transverse shear stresses from the transverse shear forces. For that purpose, the influence of the membrane forces on the transverse shear stresses was neglected and cylindrical bending displacement modes were assumed. The method also provides improved transverse shear stiffnesses. Thus, the selection of an appropriate shear correction factor is no longer necessary. In contrast to the usual method, not only equilibrium conditions, but also the material law for the transverse shear forces were used.

Brett A. Bednarcyk et al [58]

The simplified shear solution method is presented for approximating the through-thickness shear stress distribution within a composite laminate based on laminated beam theory. The method does not consider the solution of a particular boundary value problem, rather it requires only knowledge of the global shear loading, geometry, and material properties of the laminate or panel. It is thus analogous to lamination theory in that ply level stresses can be efficiently determined from global load resultants (as determined, for instance, by finite element analysis) at a given location in a structure and used to evaluate the margin of safety on a ply-by-ply basis. The simplified shear solution stress distribution is zero at free surfaces, continuous at ply boundaries, and integrates to the applied shear load.

Chapter-3

nano-CFRP HYBRID COMPOSITE

3.1 Introduction

Laminated composite materials consist of a stiff and strong micron-size phase called reinforcement, which is usually a fibrous material like a textile fabric, and another phase called matrix, which is either a polymer, a ceramic, a metal, or a carbon material. A traditional way to improve the properties of polymers and specifically increase their thermal stability and stiffness is to add micron-size fillers. However, a reduction is observed in their ductility, fracture toughness and sometimes strength.

In order to avoid those property reductions, nanocomposites can be formed by dispersing nanoparticles in the polymeric matrix: platelets like clay, fibers like carbon nanotube and carbon nanofiber, or particulates like silica or expanded graphite. A considerable improvement in the mechanical properties of the polymer matrix can be achieved with small concentrations of the particles, usually less than 5% by volume. The use of these nanoparticles could however be limited by dispersion problems and viscosity build-up related to strong inter-particle interactions.

The particle volume content plays a very important role but the interphase between the matrix and the particles plays an even major role. Among the nanoparticles, the best choice to improve the mechanical properties of the composites is to use carbon nanotubes due to their excellent mechanical, electrical, and thermal properties.



Fig.5 Schematic of nano-CFRP Hybrid Composite

3.2 Multiscale Constitutive modeling

MOC has been validated and proved efficient to model composites with infinite long fibers as well as nano fibers as reinforcements, it can be further used to model the composite material constants of hybrid nanocomposites with nano scaled carbon nano tubes and micro scaled carbon fibers as reinforcements.

Algorithm used in Multistep Homogenization for Hybrid Nanocomposite

Step1: Compute elastic moduli for composite with random nano fiber as inclusions using MOC-3D.

Step2: Compute elastic moduli for composite with agglomerated random nano fiber as inclusions using MOC-3D with agglomeration model.

Step3: Compute elastic moduli for composite with matrix properties from step1 and fiber properties from step2 using MOC-3D .

#The resulting effective moduli are taken as Matrix properties of Hybrid composite in last step.

Step4: Compute elastic moduli of composite with CFRP fiber system .

#The resulting effective moduli are taken as Fiber properties of hybrid composite in the last step.

Step5: Compute effective properties of nano-CFRP hybrid composite with Matrix properties form step3 and fiber properties form step4.

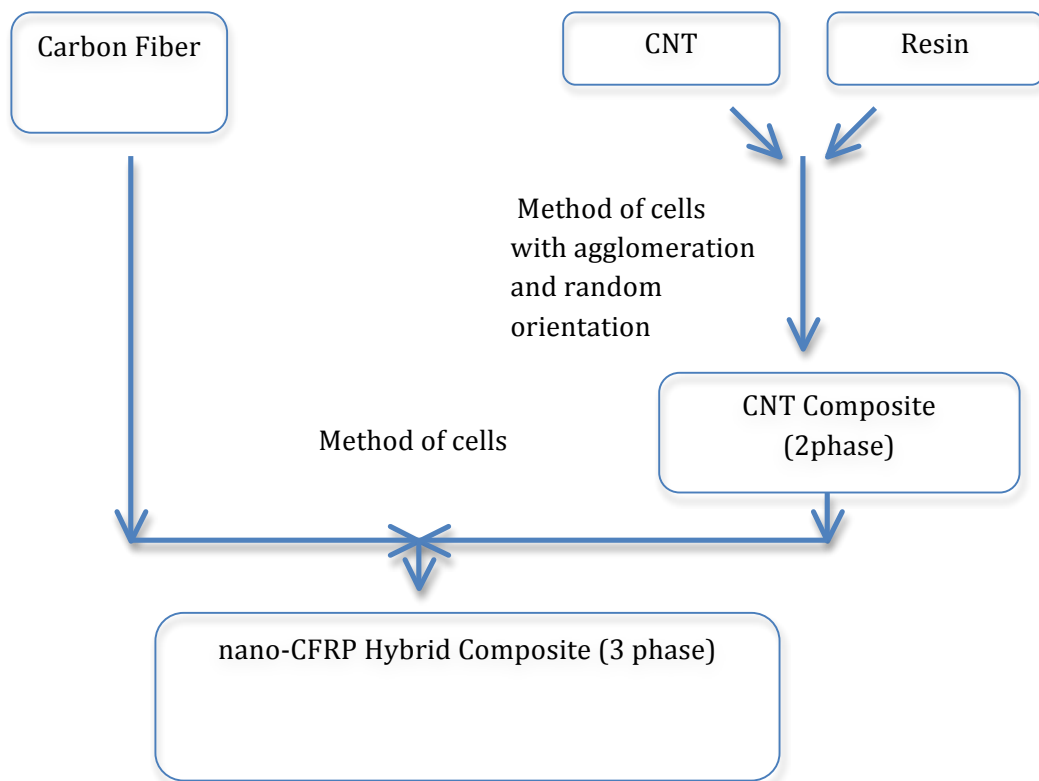


Fig.6
Flow chart representing Multistep Homogenization Scheme

Chapter-4

MULTISCALE CONSTITUTIVE MODEL VALIDATIONS

Validation 1: [55]

Material properties of Epoxy/CNT/Carbon Fiber System:

Epoxy properties:

$E_m=3.0 \text{ GPa}$, $\nu_m=0.3$

CNT properties:

$E_{cnt}=1000 \text{ GPa}$, length of CNT (l)= 100 nm, diameter of CNT (d)= 10 nm, $\nu_f=0.3$

Carbon Fiber properties:

$E_a=294 \text{ GPa}$, $E_t=18.5 \text{ GPa}$, $\nu_a=0.27$, $\nu_t=0.3$, $G=25 \text{ GPa}$

Results:

$E_{MOC-Hybrid} = 8.29$ (Transverse modulus)

$E_{Exp} = 10.02$ (deviation=17.26 %)

$E_{th} = 13.93$

Table 1. Validation of Epoxy/CNT/Carbon Fiber System

Validation:2 [54]

Material properties of Epoxy/CNT/Carbon Fiber System:

Epoxy properties:

$E_m=2.72.0 \text{ GPa}$, $\nu_m=0.33$

CNT properties:

SWCNT:

$E_{cnt}=640 \text{ GPa}$, length of CNT (l)= $25\mu\text{m}$, diameter of CNT (d)= 1.4nm , $\nu_f=0.3$

$\rho=1350\text{kg/m}^3$ wt%=.2

MWCNT:

$E_{cnt}=400 \text{ GPa}$, length of CNT (l)= $50\mu\text{m}$, diameter of CNT (d)= 20nm , $\nu_f=0.3$

$\rho=1350\text{kg/m}^3$ wt%=.1

Carbon Fiber properties:

$E_a=294 \text{ GPa}$, $E_t=18.5 \text{ GPa}$, $\nu_a=0.27$, $\nu_t=0.3$, $G=25 \text{ GPa}$

Results:

$E_{MOC-Hybrid} = 235.81 \text{ (Longitudinal modulus)}$

$E_{th} = 221.4 \text{ (deviation= 6.50%)}$

Table 2. Validation of Epoxy/CNT/Carbon Fiber System

Material properties of Epoxy/CNT:

Epoxy properties:

$E_m = 2.59 \text{ GPa}$, $\nu_m = 0.3$ $\rho = 1200 \text{ kg/m}^3$

CNT properties:

SWCNT:

$E_{cnt} = 1000 \text{ GPa}$, length of CNT (l)= $30\mu\text{m}$, diameter of CNT (d)= 2 nm , $\nu_f = 0.33$

$\rho = 2100 \text{ kg/m}^3$ wt%=.1

DWCNT:

$E_{cnt} = 1000 \text{ GPa}$, length of CNT (l)= $30\mu\text{m}$, diameter of CNT (d)= 2.8 nm , $\nu_f = 0.33$

$\rho = 2100 \text{ kg/m}^3$ wt%=.3

MWCNT:

$E_{cnt} = 1000 \text{ GPa}$, length of CNT (l)= $50\mu\text{m}$, diameter of CNT (d)= 15 nm , $\nu_f = 0.33$

$\rho = 2100 \text{ kg/m}^3$ wt%=.3

Results:

SWCNT:

$E_{MOC-Hybrid} = 2.763$

$E_{exp} = 2.691$ (deviation= 2.67 %)

DWCNT:

$E_{MOC-Hybrid} = 3.099$

$E_{exp} = 2.885$ (deviation= 7.417%)

MWCNT:

$E_{MOC-Hybrid} = 2.844$

$E_{exp} = 2.765$ (deviation= 2.80%)

Validation : 3[59]

Table 3. Validation of Epoxy/CNT System

Validation 4: [60]

Material properties of Epoxy/Carbon Fiber System:
<u>Epoxy properties:</u>
$E_m=3.0 \text{ GPa}$, $\nu_m=0.3$
<u>Carbon Fiber properties:</u>
$E_a=230 \text{ GPa}$, $E_t=8 \text{ GPa}$, $\nu=0.256$, $G=27.3 \text{ GPa}$ $V_f=.502$
Results:
$E_{MOC-Hybrid} = 116.96 \text{ (longitudinal modulus)}$
$E_{MOC-Hybrid} = 7.28 \text{ (transverse modulus)}$
$E_{Exp(L)} = 117$
$E_{Exp(T)} = 7.02 \text{ (deviation}=3.71 \text{ %)}$

Table 4. Validation of Epoxy/ Carbon Fiber System

Chapter-5

SIMULATIONS OF nano-CFRP

5.1 Simulations

1. CFRP composites with CNTs aligned in longitudinal direction

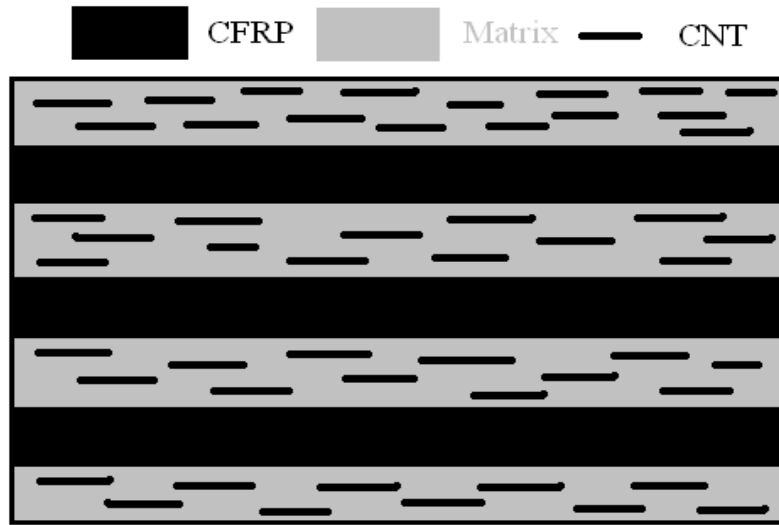


Fig. 7

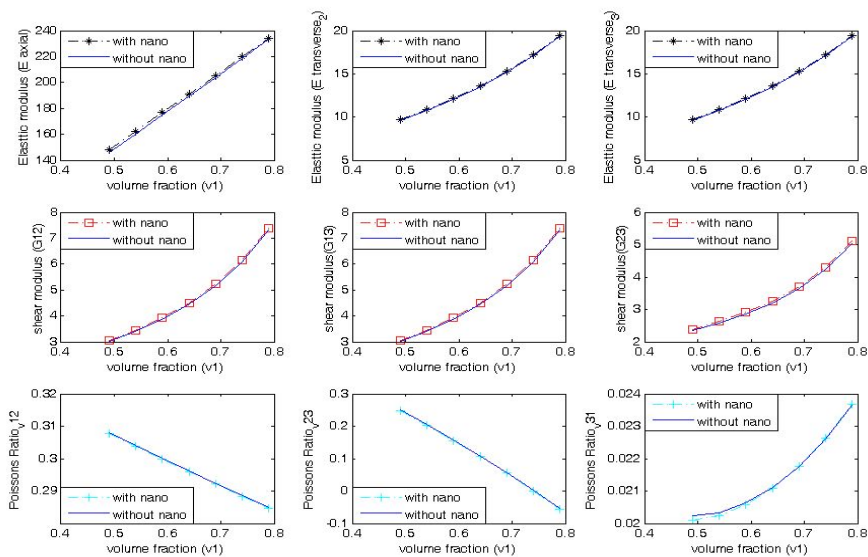


Fig. 8 Elastic constants at wt% = 2.0 & Aspect Ratio = 1000

2.CFRP composites with CNTs aligned in transverse direction

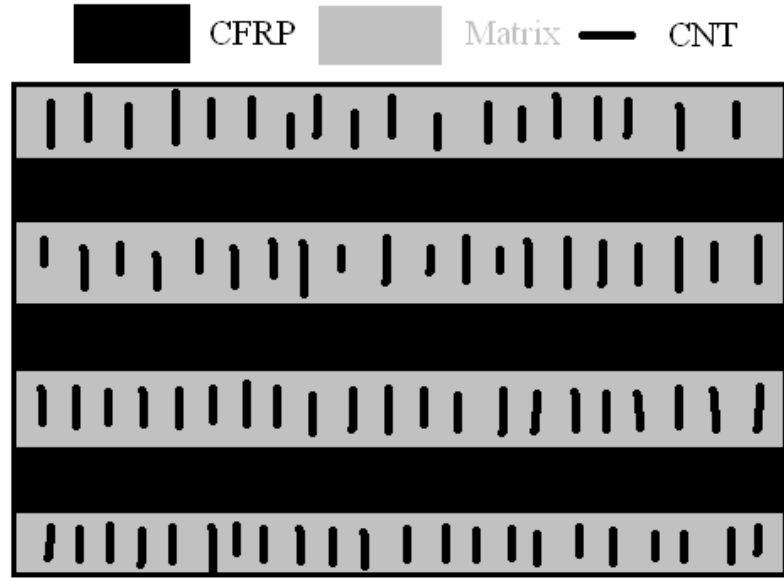


Fig.9

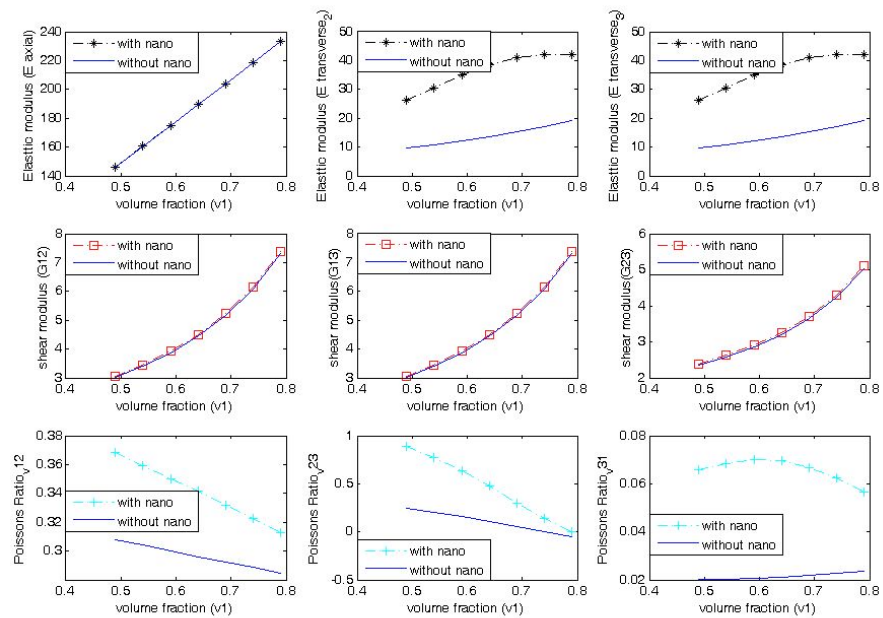


Fig. 10 Elastic constants at wt% = 2.0 & Aspect Ratio = 1000

3. CFRP composites with randomly oriented CNTs

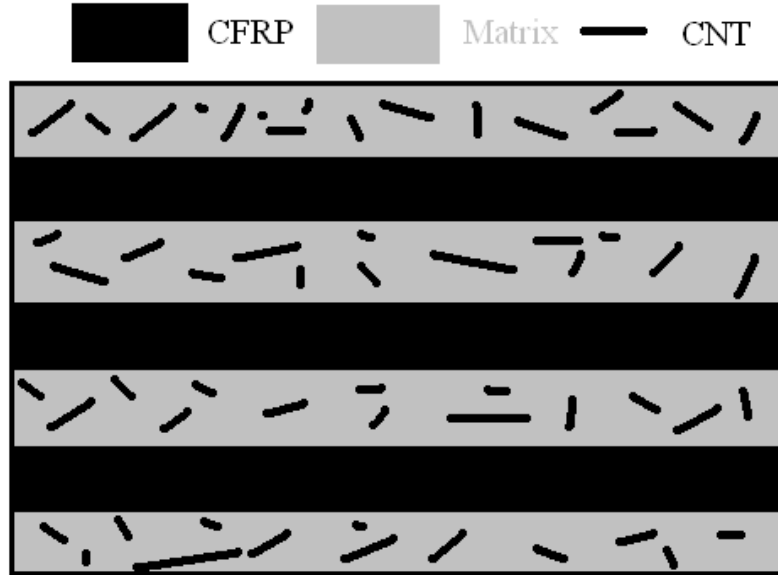


Fig.11

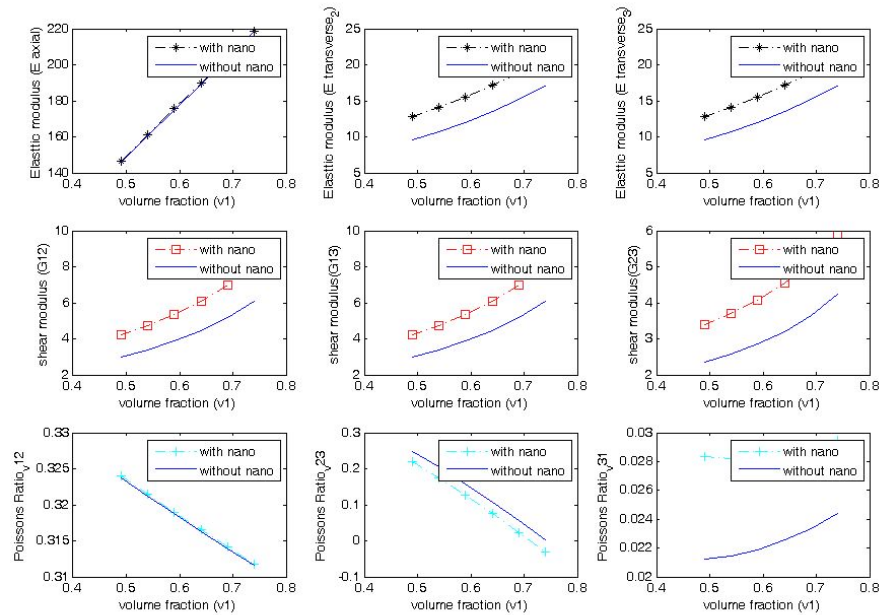


Fig.12 Elastic constants at wt% = 2.0 & Aspect Ratio = 1000

5.2 Observations from simulations

Case 1: CFRP with CNTs aligned in longitudinal direction

- With CNTs aligned in longitudinal direction, there is no significant change in elastic constants because the properties are fiber dominated
- The material is transversely isotropic

Case 2: CFRP with CNTs aligned in transverse direction

- With CNTs aligned in transverse direction, there is significant improvement in transverse modulus
- At a particular volume fraction of CF and/or particular weight percentage or aspect ratio of CNT, transverse modulus starts to deteriorate
- The material is transversely isotropic

Case 3: CFRP with randomly oriented CNTs

- There is significant increase in transverse and shear modulus with randomly oriented CNT inclusions
- The material is transversely isotropic

Chapter-6

COMPOSITE LAMINATES

6.1 Introduction

A real structure will not consist of a single lamina but a laminate consisting of more than one lamina bonded together through their thickness since lamina thicknesses are on the order of 0.005 in. (0.125 mm), implying that several laminae will be required to take realistic loads (a typical glass/epoxy lamina will fail at about only [131,350 N/m] width of a normal load along the fibers). Also the mechanical properties of a typical unidirectional lamina are severely limited in the transverse direction. A laminate stacked several unidirectional layers may be an optimum laminate for unidirectional loads. However, for complex loading and stiffness requirements, this would not be desirable. This problem can be overcome by making a laminate with layers stacked at different angles for given loading and stiffness requirements. This approach increases the cost and weight of the laminate and thus it is necessary to optimize the ply angles. Moreover, layers of different composite material systems may be used to develop a more optimum laminate.

A laminate is made of a group of single layers bonded to each other. Each layer can be identified by its location in the laminate, its material, and its angle of orientation with a reference axis. Each lamina is represented by the angle of ply and separated from other plies by a slash sign. The first ply is the top ply of the laminate.

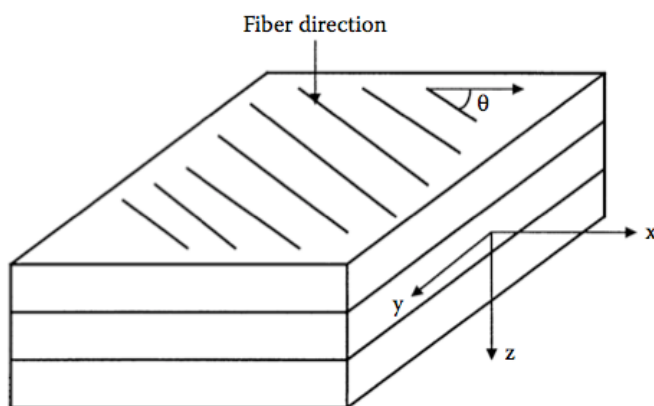


Fig.13 Schematic of Laminate

6.2 Laminate Theory[61]

In order to calculate the effective moduli of a composite laminate system such as nano-CFRP hybrid laminate, the mechanics of the system needs to be understood.

For a 2-d lamina under axial load and bending moments

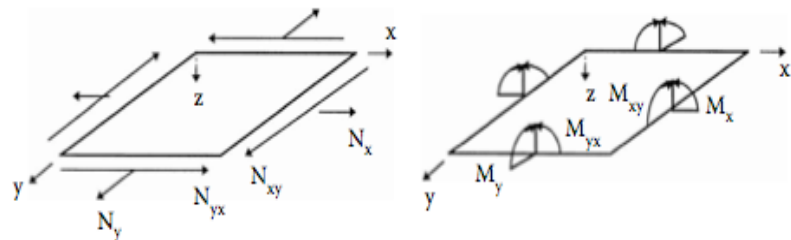


fig.14

Strain–displacement Relations for a Laminate

$$\begin{bmatrix} \frac{N}{M} \end{bmatrix} = \begin{bmatrix} A & B \\ B & D \end{bmatrix} \begin{bmatrix} \frac{\varepsilon^0}{K} \end{bmatrix} = \begin{bmatrix} \varepsilon_x^0 \\ \varepsilon_y^0 \\ \gamma_{xy}^0 \end{bmatrix} + Z \begin{bmatrix} k_x \\ k_y \\ k_{xy} \end{bmatrix}$$

Strain and Stress

$$\begin{bmatrix} \sigma_x \\ \sigma_y \\ \tau_{xy} \end{bmatrix} = \begin{bmatrix} \bar{Q}_{11} \bar{Q}_{12} \bar{Q}_{16} \\ \bar{Q}_{12} \bar{Q}_{22} \bar{Q}_{26} \\ \bar{Q}_{16} \bar{Q}_{26} \bar{Q}_{66} \end{bmatrix} \begin{bmatrix} \varepsilon_x \\ \varepsilon_y \\ \gamma_{xy} \end{bmatrix}$$

where \bar{Q} the transformed reduced stiffness matrix.

From above equations

$$\begin{bmatrix} \sigma_x \\ \sigma_y \\ \tau_{xy} \end{bmatrix} = \begin{bmatrix} \bar{Q}_{11} \bar{Q}_{12} \bar{Q}_{16} \\ \bar{Q}_{12} \bar{Q}_{22} \bar{Q}_{26} \\ \bar{Q}_{16} \bar{Q}_{26} \bar{Q}_{66} \end{bmatrix} \begin{bmatrix} \varepsilon_x^0 \\ \varepsilon_y^0 \\ \gamma_{xy}^0 \end{bmatrix} + \begin{bmatrix} \bar{Q}_{11} \bar{Q}_{12} \bar{Q}_{16} \\ \bar{Q}_{12} \bar{Q}_{22} \bar{Q}_{26} \\ \bar{Q}_{16} \bar{Q}_{26} \bar{Q}_{66} \end{bmatrix} Z \begin{bmatrix} k_x \\ k_y \\ k_{xy} \end{bmatrix}$$

The strains vary linearly only through the thickness of each lamina. The stresses, however, may jump from lamina to lamina because the transformed reduced-stiffness matrix [Q] changes from ply to ply because [Q] depends on the material and orientation of the ply.

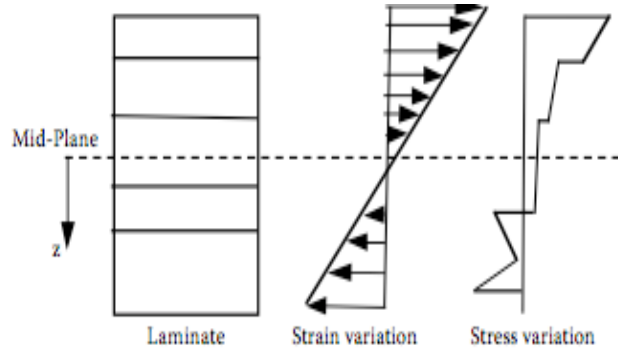


Fig.15 Variation of stress and strain in a laminate with respect to distance from midplane

Force and Moment Resultants Related to Midplane Strains and Curvatures:

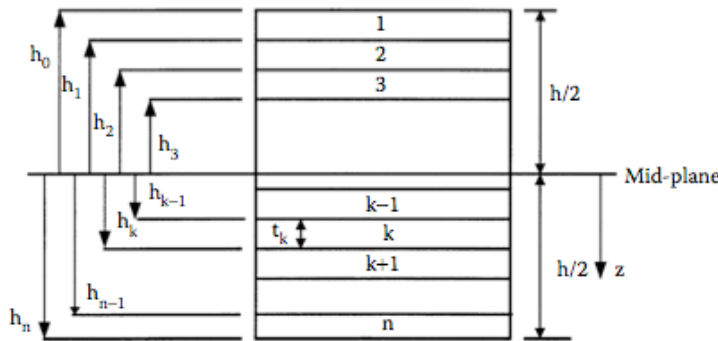


fig.16 Convention for height of laminate from midplane

The following relation holds good

$$\begin{bmatrix} N_x \\ N_y \\ N_{xy} \\ M_x \\ M_y \\ M_{xy} \end{bmatrix} = \begin{bmatrix} A_{11}A_{12}A_{16}B_{11}B_{12}B_{16} \\ A_{12}A_{22}A_{26}B_{12}B_{22}B_{26} \\ A_{16}A_{26}A_{66}B_{16}B_{26}B_{66} \\ B_{11}B_{12}B_{16}D_{11}D_{12}D_{16} \\ B_{12}B_{22}B_{26}D_{12}D_{22}D_{26} \\ B_{16}B_{26}B_{66}D_{16}D_{26}D_{66} \end{bmatrix} \begin{bmatrix} \epsilon_x^0 \\ \epsilon_y^0 \\ \gamma_{xy}^0 \\ k_x \\ k_y \\ k_{xy} \end{bmatrix}$$

where [A], [B], and [D] matrices are called the extensional, coupling, and bending stiffness matrices, respectively.

$$A_{ij} = \sum_{k=1}^n [(\bar{Q}_{ij})]_k (h_k - h_{k-1}), i=1,2,6; j=1,2,6$$

$$B_{ij} = \frac{1}{2} \sum_{k=1}^n [(\bar{Q}_{ij})]_k (h_k^2 - h_{k-1}^2), i=1,2,6; j=1,2,6$$

$$D_{ij} = \frac{1}{3} \sum_{k=1}^n [(\bar{Q}_{ij})]_k (h_k^3 - h_{k-1}^3), i=1,2,6; j=1,2,6$$

In short form the laminate engineering constants are written in the form of **ABD** matrix as below.

$$\begin{bmatrix} N \\ M \end{bmatrix} = \begin{bmatrix} A & B \\ B & D \end{bmatrix} \begin{bmatrix} \varepsilon^0 \\ K \end{bmatrix}$$

Special case : Symmetric Laminate

Only for a special case of symmetric laminate the inplane effective moduli can be calculated, since the coupling matrix vanishes.

$$E_x = \frac{1}{hA_{11}^*}$$

$$E_y = \frac{1}{hA_{22}^*}$$

$$G_{xy} = \frac{1}{hA_{66}^*}$$

$$V_{xy} = -\frac{A_{12}^*}{A_{11}^{&*}}$$

$$V_{yx} = -\frac{A_{12}^*}{A_{22}^{&*}}$$

where $[A^*] = A^{-1}$.

6.3 Simulations of nano-CFRP hybrid Composite Laminates

CFRP laminates have been extensively used for Aerospace and Automobile applications because their high mechanical properties. But these Prepregs have poor out of plane properties due to the transversely isotropic Nature of carbon fibers.

With an aim of Enhancing Transverse plane properties E_{22}, G_{12}, V_{12} combinations of the various parameters like types of inclusions , orientation of lamina , lamina order were carried out and objective conclusions have been reached.

Common Inputs:

CFRP: 70%

CNT: 1%

a/r :1000 i.e., l=1um,d=1nm

Thickness=5mm(lamina)

3lamina- laminate system

Nomenclature:

Orientation 1: (ort-1)

Top lamina: angle =(0:5:90)

Middle lamina: angle=0

Bottom lamina: angle=(0:5:90)

Orientation 2: (ort-2)

Top lamina: angle =0

Middle lamina: angle=(0:5:90)

Bottom lamina: angle=0

Type of Lamina

- 1- CFRP with longitudinally aligned cnt
- 2- CFRP with transversely aligned cnt
- 3- CFRP with Randomly oriented cnt

Example: laminate 121

Top lamina= CFRP with longitudinally aligned cnt

Middle lamina= CFRP with transversely aligned cnt

Bottom lamina= CFRP with Randomly oriented cnt

Type: 111

Ort1

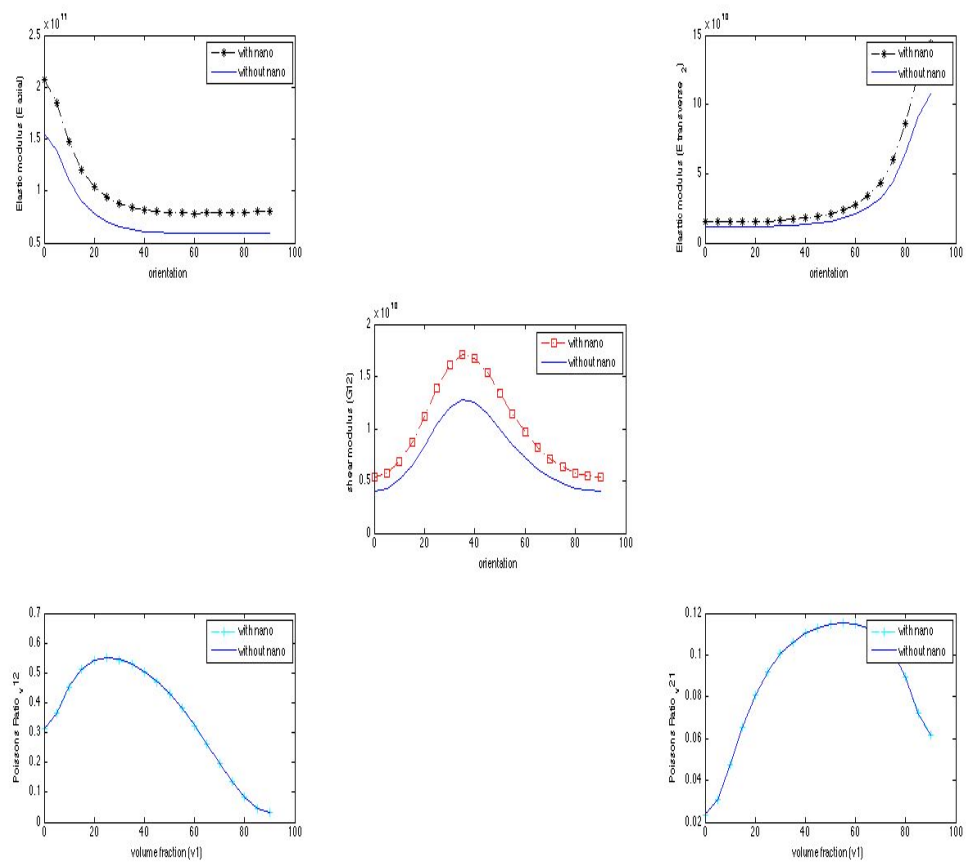


Fig.17 case 111-Ort1

Type: 222

Ort1

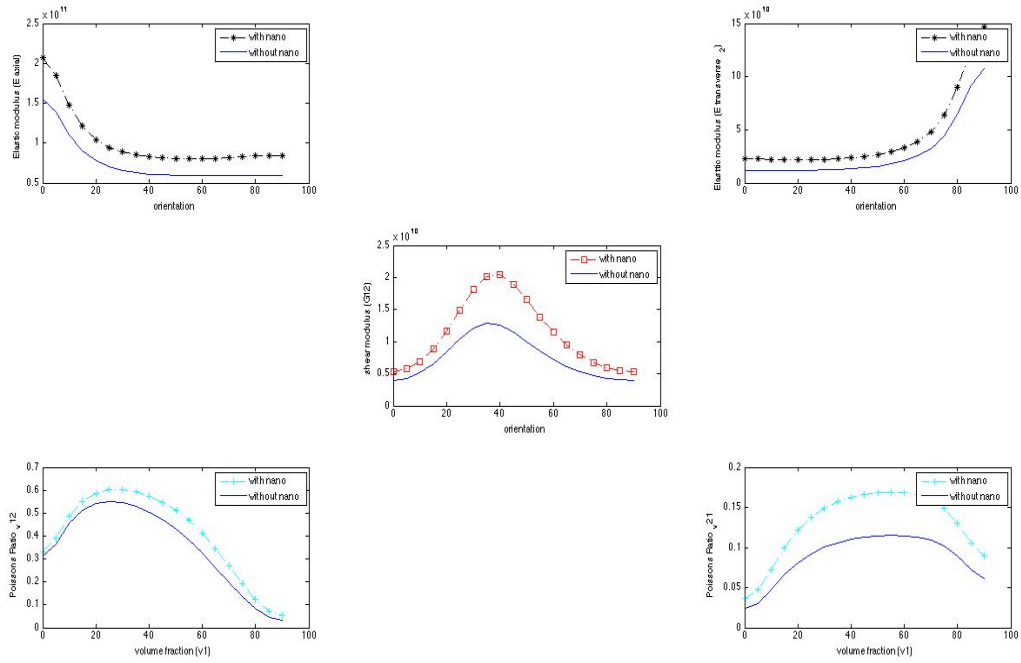


Fig.18 case 222-Ort1

Type222

Ort2

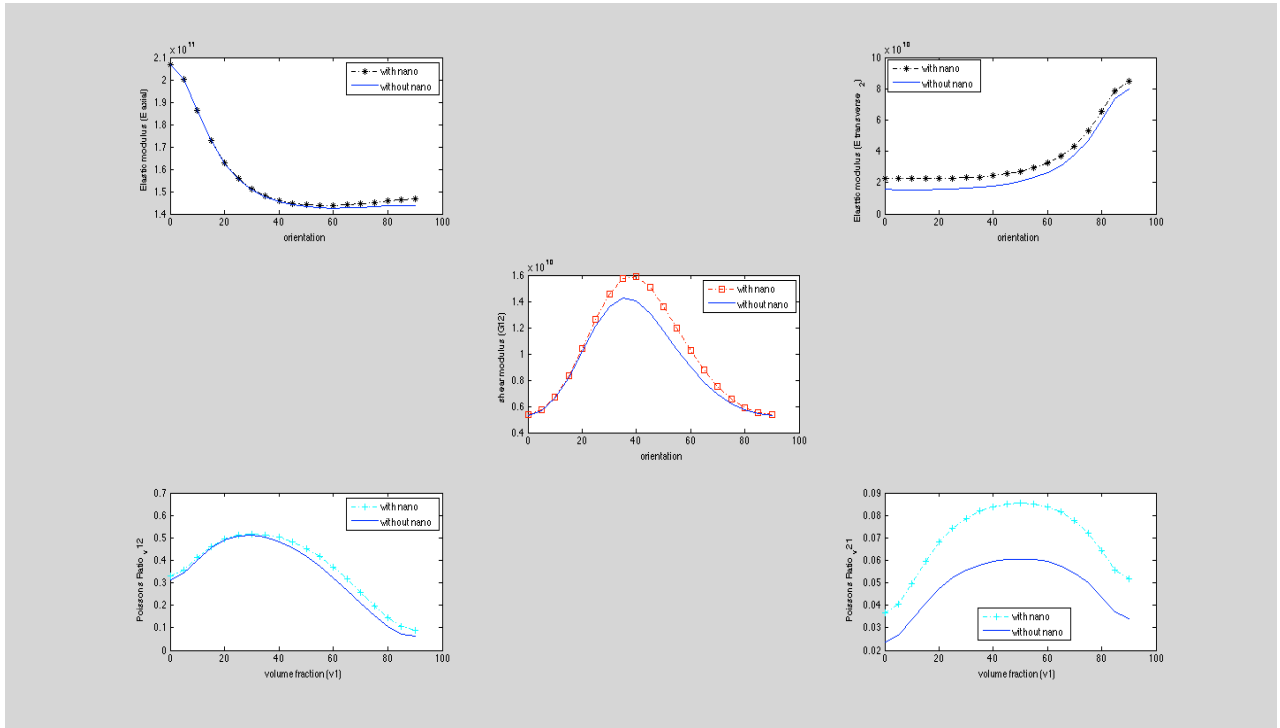


Fig.19 case 222-Ort2

Conclusions:

Out of the total 9 combinations totally possible the above critical ones were selected and reported.

1. We can observe from fig.17 that Maximum value of young's modulus occurs at 35deg in contrast to 45deg for isotropic plies. This can be explained because of the transversely isotropic Nature of Long fibers in the composite.
2. If improvement only in E_{22} is desired from fig.19 its clear that 222-o2(38% improvement) is best scenario.
3. If improvement only in G_{12} is desired from fig.18 its clear that 222-o1(17% improvement) is best scenario.
4. If improvement in both E_{22} and G_{12} is desired from fig.18 its clear that 222-o1(33%,17% improvement) is best scenario.

Chapter-7

INTERLAMINAR SHEAR STRESS

7.1 Introduction

A commonly observed failure mode in laminated composite materials is the delamination between the composite layers. Delamination may develop during manufacture due to incomplete curing or may result from the interlaminar stresses created by impact/load.

By employing lamination theory, one can determine the in-plane stress distribution in each layer of a laminate from the knowledge of the applied force and moment resultants. This information enables determination of ply-by-ply margins for the laminate, which are needed for design and sizing. The distributions of the interlaminar shear stresses in each layer from the applied shear resultants are not readily available from the standard lamination theory equations. These stresses are also needed to enable design and sizing of laminates subjected to global shear loads.

A analytical method called Simplified Shear Model based on laminated beam theory with shear loading, for determining the interlaminar shear stress distribution in a laminate from a given applied shear resultant is followed[58]. It should be emphasized that the classical or the higher-order (e.g., first-order shear deformable) plate theory cannot be employed to determine the correct interlaminar shear stress distribution through the laminate thickness from the knowledge of the force, moment, and shear resultants. Indeed, the classical plate theory provides identically zero interlaminar shear stresses, whereas the higher-order plate theories provide piece-wise profiles that are discontinuous at the ply interfaces.

It should also be noted that the simple shear solution does not involve the solution of a particular boundary value problem. Rather, it is only assumed that the force, moment, and shear resultants are known at a particular location in the laminate, and the solution is independent of the source of these known resultant quantities. Conversely, in order to obtain the interlaminar shear distribution via integration of the differential equations of equilibrium, the solution of a boundary value problem would be required to determine the variation of the stress fields in each ply.

7.2 Modeling the ILSS: Simplified Shear Model

To determine the distribution of the shear stress in a laminate given the global applied shear resultant, Q a laminate (fig. xx) With a applied shear force P consisting of N layers is considered, with the layer number denoted by k . Following the concept of a composite beam Beer and Johnston [], the actual laminate cross-section is replaced with an effective cross-section. As shown in fig. xx, the original width of each layer (b) is transformed to $b n_k$, where,

$$n_k = \frac{E_x^k}{\bar{E}_x}$$

E_x^k is the Young's modulus of layer k in the x -direction, and \bar{E}_x is the average Young's modulus of the laminate in the x -direction. \bar{E}_x Serves only as a normalization factor, which allows the ply stiffnesses to be scaled with respect to each other. Alternatively, the Young's modulus of one particular ply may be used. In bending, under a plane strain condition, where, $\varepsilon_y = 0$, E_x^k should be modified to

$$E_x^k = E_x^k / [1 - V_{xy}^k V_{yx}^k] \text{ [ref]}$$

The neutral axis for the laminate is located at the centroid of the transformed laminate cross-section and is given (with respect to the laminate midplane coordinate system) by,

$$Z^* = \frac{\sum_{k=1}^N \frac{1}{2} (Z_k + Z_{k-1}) t_k n_k}{\sum_{k=1}^N t_k n_k}$$

where A_k and t_k are the area and thickness of layer k , respectively. The distance of a point from the neutral axis is denoted by $\hat{Z} = Z - Z^*$

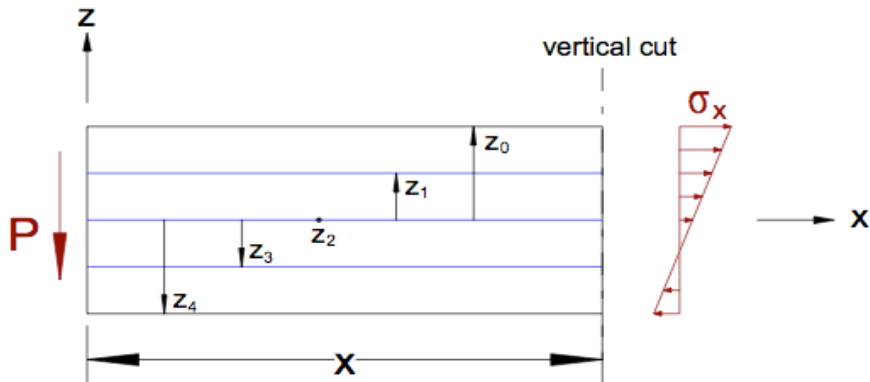


Fig.20—Portion of a laminate subjected to a shear force, P , and the resulting normal stress distribution on an arbitrary cross-section.

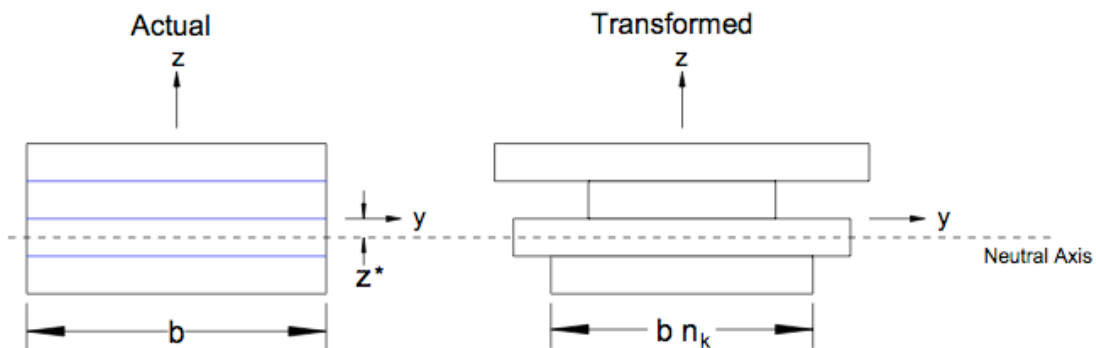


Fig. 21 Original (actual) and transformed laminate cross-sections.

The applied shear loading causes a normal stress distribution at an arbitrary vertical cross-section given according to beam theory Beer and Johnston [ref] by

$$\sigma_x = -\frac{M \hat{Z}}{I}$$

where I is the moment of inertia of the transformed laminate cross-section (fig. 2) and M is moment at the vertical cross-section. Because a counter clockwise moment is considered positive, equilibrium dictates that $M = -Px$, thus,

$$\sigma_x = -\frac{Px \hat{Z}}{I}$$

To obtain the shear force, denoted by H , acting on an arbitrary horizontal cross-section at location $\hat{Z} = \hat{Z}_c$, within ply number k (see fig. 3), consider the equilibrium of forces in the x -direction, which requires,

$$-H + \int \sigma_x dA = 0$$

where dA is the area of the differential element indicated in figure 3. Note that the positive H sign convention indicated in figure 3 is consistent with that employed by Beer and Johnston (ref). Thus we get

$$H = \frac{Px}{I} \int_{\hat{Z}_N}^{\hat{Z}_c} \hat{Z} dA$$

where $C = \hat{Z}_N$ denotes the distance from the neutral axis to the bottom surface of the laminate. Using $dA = bn_k d\hat{z}$

$$H = \frac{Px}{I} \int_{\hat{Z}_N}^{\hat{Z}_c} bn_k \hat{Z} d\hat{z}$$

The integral appearing, which is denoted by $Q^l(k, \hat{z})$ can be decomposed as follows,

$$Q^l(k, \hat{z}) = \int_{\hat{Z}_N}^{\hat{Z}_c} bn_k \hat{Z} d\hat{z} = \int_{\hat{Z}_k}^{\hat{Z}_c} bn_k \hat{Z} d\hat{z} + \int_{\hat{Z}_{k+1}}^{\hat{Z}_k} bn_{k+1} \hat{Z} d\hat{z} + \dots + \int_{\hat{Z}_N}^{\hat{Z}_{N-1}} bn_N \hat{Z} d\hat{z}$$

It follows that

$$Q^l(k, \hat{z}) = \frac{bn_k}{2} (\hat{Z}_c - \hat{Z}_k)^2 + \frac{1}{2} \sum_{m=k+1}^N bn_m (\hat{Z}_{m-1} - \hat{Z}_m)^2$$

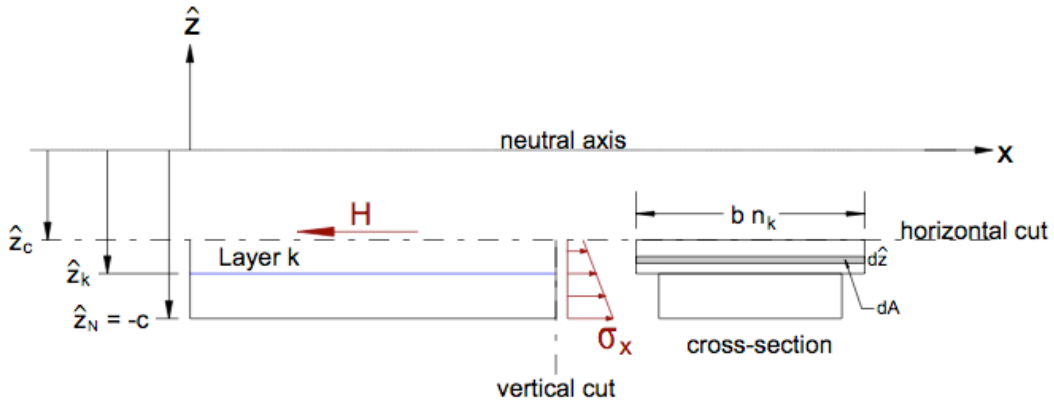


Figure. 22—Section of laminate acted upon by the horizontal shear force, H , and the distributed normal stress

where $Z_N = -C$. Hence, the shear force, H , is given by,

$$H = \frac{Px}{I} Q^l(k, \hat{z})$$

The shear stress, τ , is given by,

$$\tau = -\frac{H}{xb}$$

where the negative sign is due to the opposite directionality of the internal shear force compared to the shear stress (see app. B). The applied shear resultant Q is related to the applied shear force P , by $Q = P/b$, and it follows that,

$$\tau(k, \hat{Z}) = -\frac{Q}{I} Q^l(k, \hat{z})$$

employing this equation, the moment of inertia of the transformed beam cross-section is given by,

$$I = \sum_{k=1}^N \left[\frac{1}{12} b n_k t_k^3 + b n_k t_k \left(\frac{Z_k + Z_{k-1}}{2} \right)^2 \right]$$

Thus with given above equations the shear stress distribution throughout the laminate can be determined.

7.3 Validations of ILSS

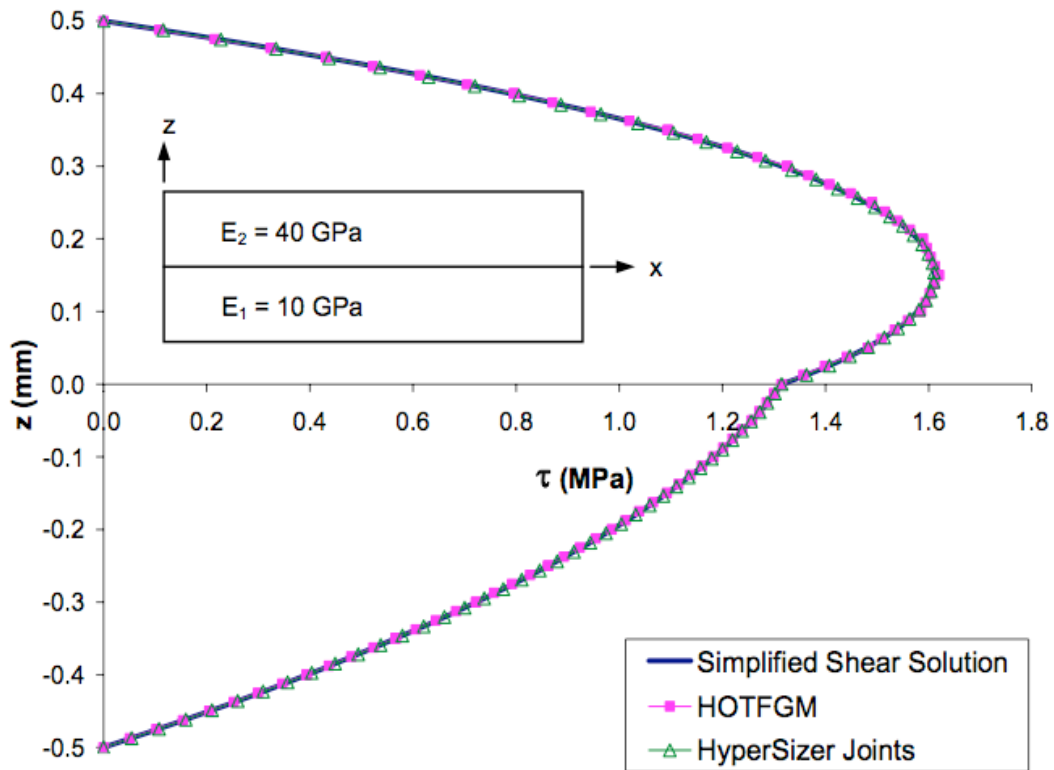


Fig.23 Distribution of ILSS with thickness : Brett A. Bednarcyk et al

$E=[40\text{Mpa} \ 10\text{Mpa}] \ v=[.3 \ .3] \ \text{Thickness}=[.5\text{mm} \ .5\text{mm}]$

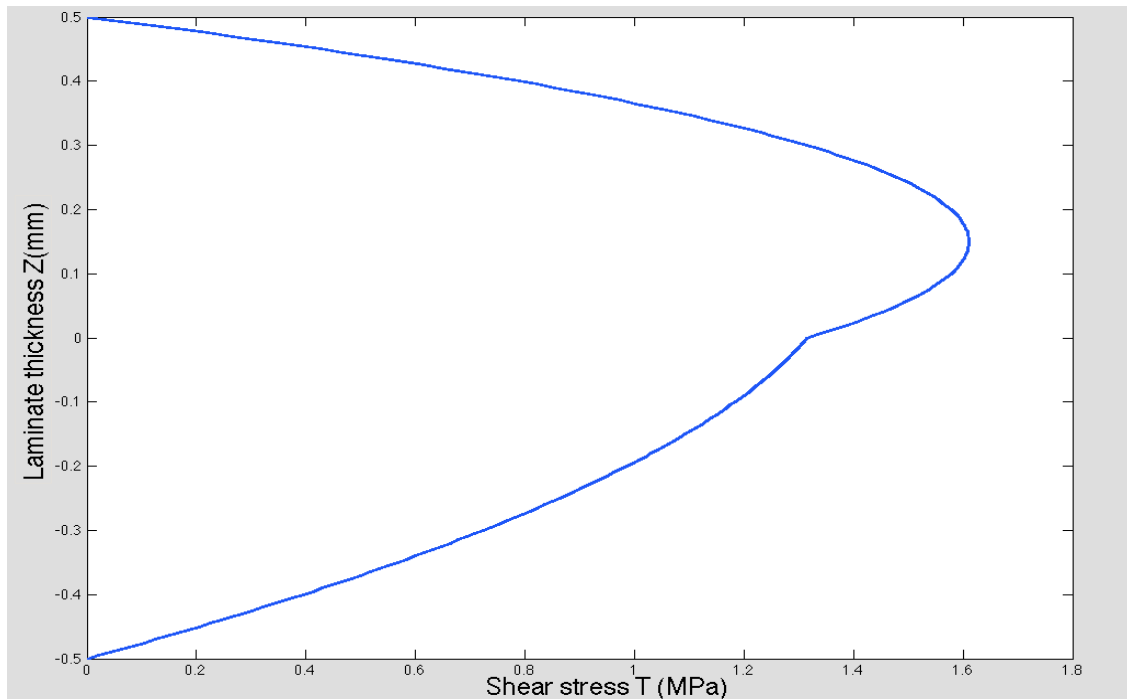


Fig.24 Distribution of ILSS with thickness modeled in Matlab

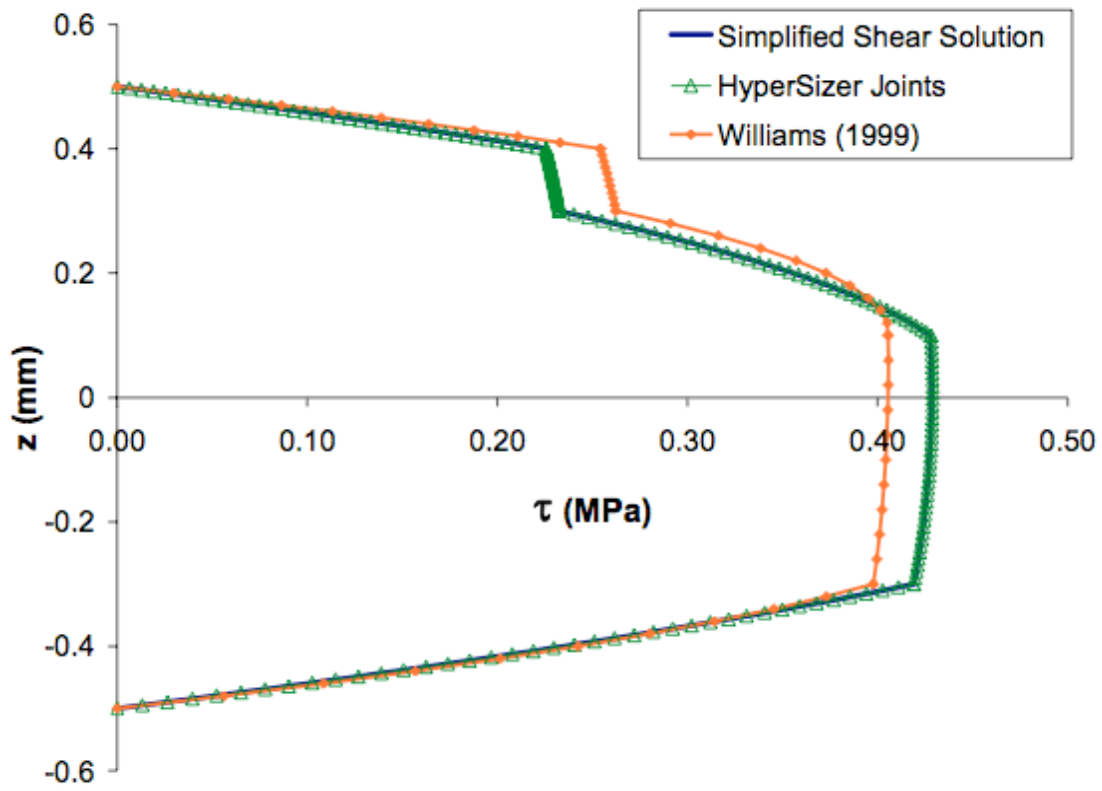


Fig.25 Distribution of ILSS with thickness : Brett A. Bednarcyk et al

$E=[25 \ 1 \ 25 \ 1 \ 25]$ Mpa $v=[.25 \ .1 \ .25 \ .1 \ .25]$ Thickness=[.1 .1 .2 .4 .2]mm

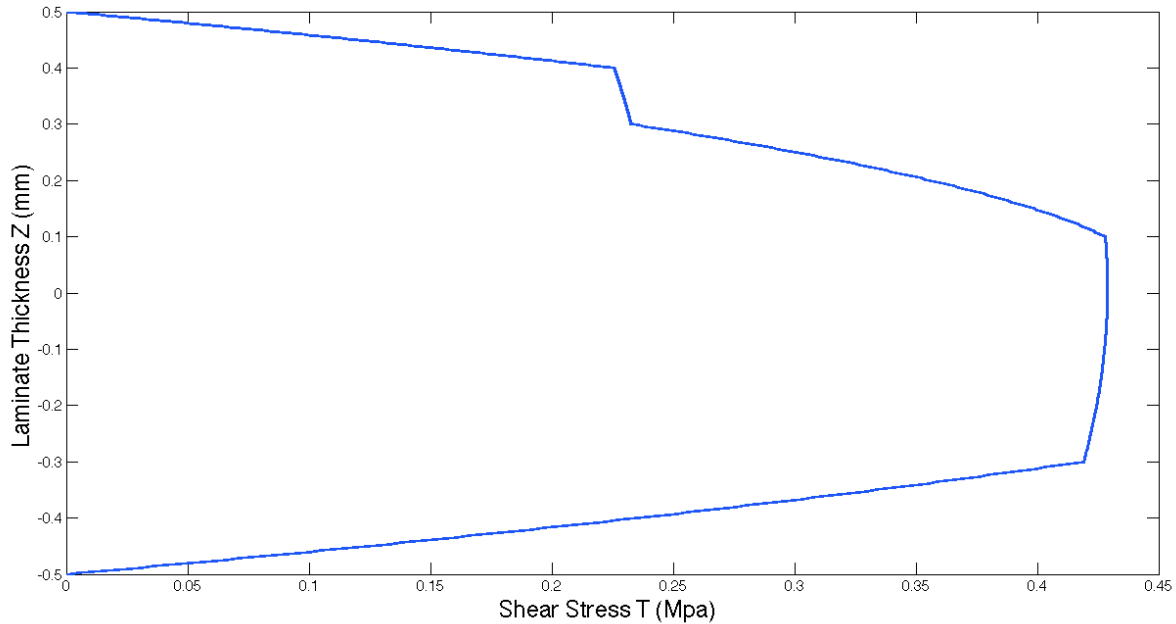


Fig.26 Distribution of ILSS with thickness modeled in Matlab

7.4 Damage Tolerant Laminates with Cnt inclusion

Engineering Design optimizes the thickness, orientation for study of deflection, frequency and failure criteria .To enhance mechanical properties of a laminate system and to meet design requirements, parameters like thickness, number of lamina and orientation of plies are manipulated. In this report a Novel method is introduced to enhance the ILSS thus making them damage tolerant by reinforcing CFRP plies with Cnts without increasing number of layers or thickness of plies.

7.5 Simulations

Parameters:

1. Number of lamina =3
2. Thickness of lamina = .5 mm each
3. Wt% =1& 2% of cnt inclusion in each lamina
4. Lamina Orientation (combinations of 0,45,90 deg orientations)
 $[0\ 0\ 0]$ $[0\ 45\ 0]$ $[45\ 0\ 45]$ $[45\ 90\ 45]$ $[90\ 45\ 90]$ $[90\ 0\ 90]$ $[0\ 90\ 0]$ $[45\ 45\ 45]$
 $[90\ 90\ 90]$
5. Order of Lamina in Laminate
 $[\text{cfrp}\ \text{nano-cfrp}\ \text{cfrp}]$ $[\text{nano-cfrp}\ \text{cfrp}\ \text{nano-cfrp}]$ $[\text{nano-cfrp}\ \text{nano-cfrp}\ \text{nano-cfrp}]$
6. Load applied is 1Mpa in Y-direction.

Simulations were done for all combinations of above parameters and Interlaminar shear stress T_{yz} Distribution of only significant cases are presented .

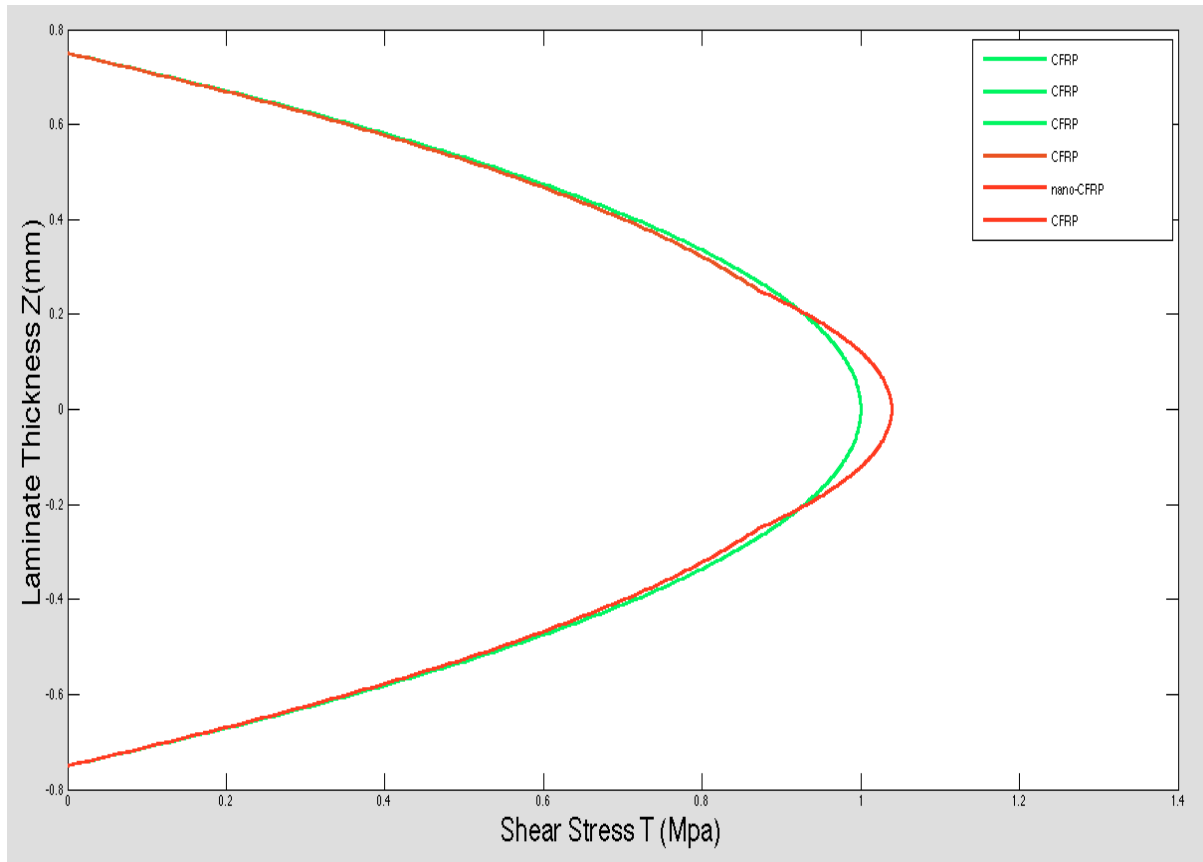


fig.27 T_{yz} Distribution of 0-0-0 [cfrp nano-cfrp cfrp]

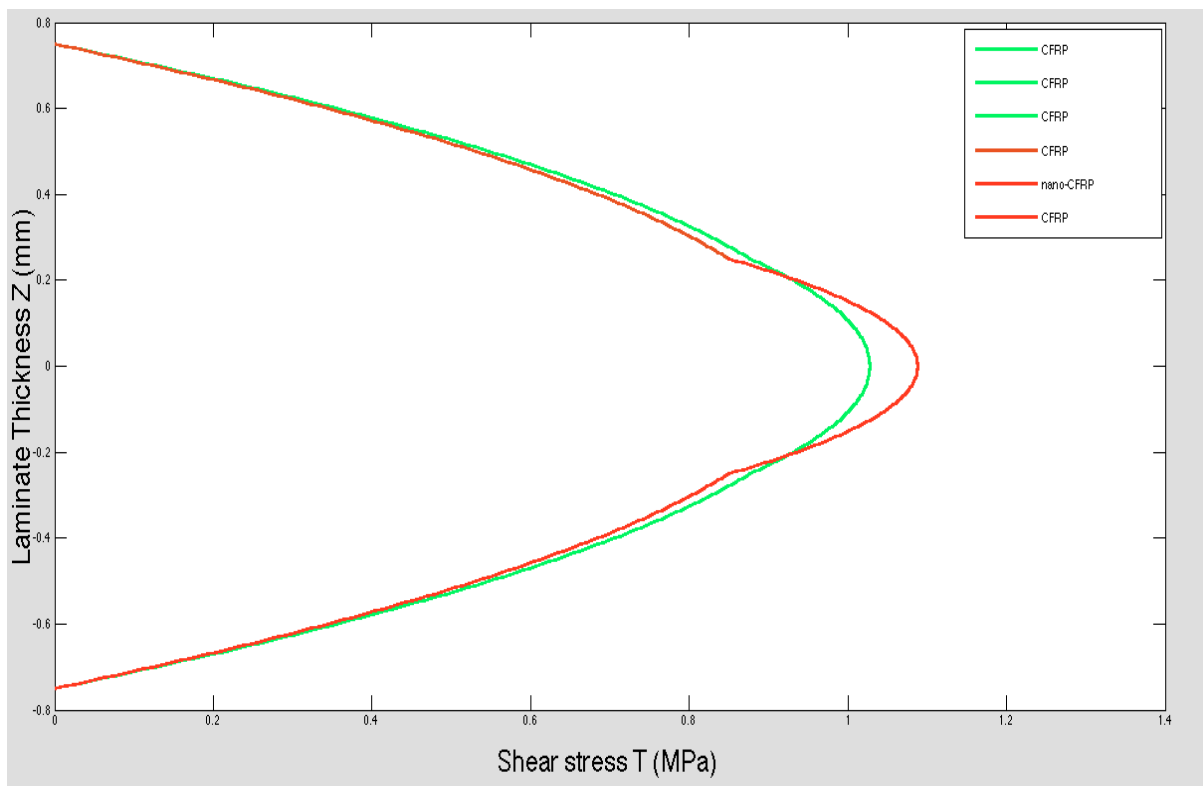


fig.28 T_{yz} Distribution of 0-45-0 [cfrp nano-cfrp cfrp]

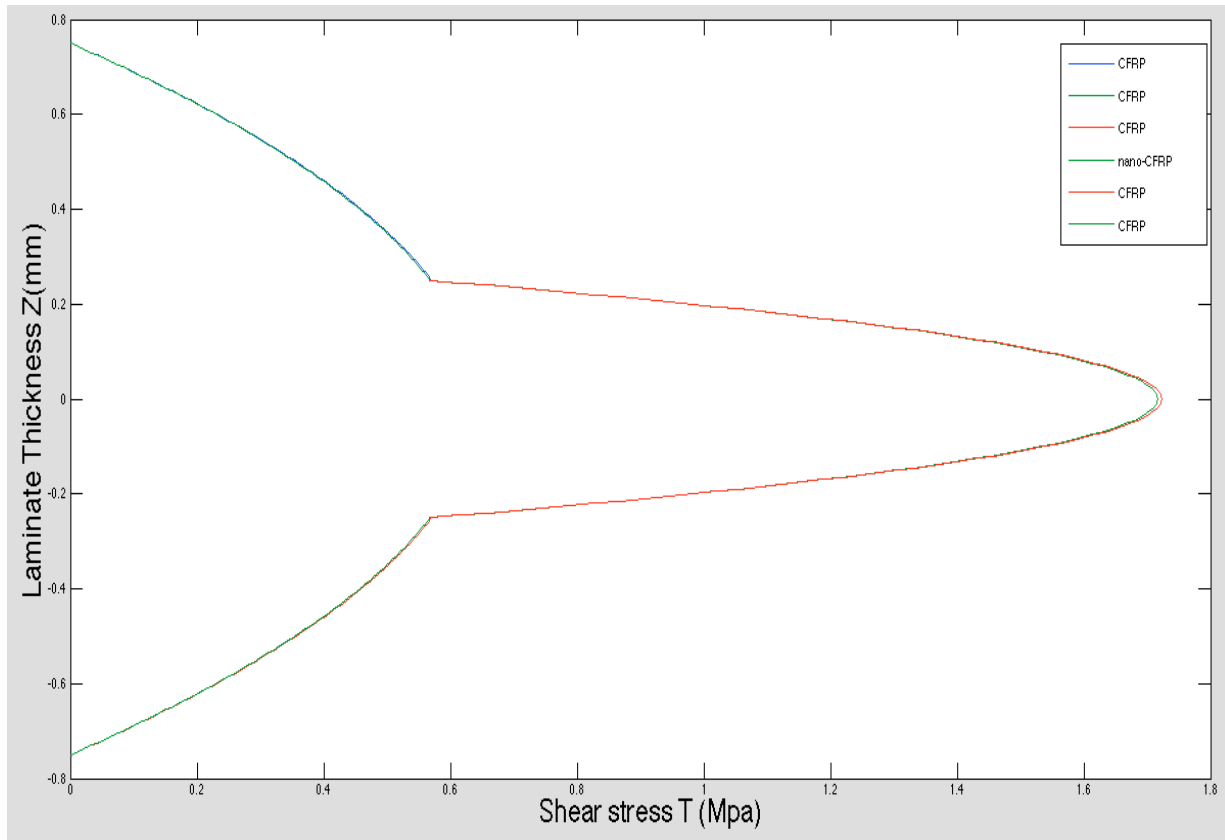


fig.29 T_{yz} Distribution of 0-90-0 [cfrp nano-cfrp cfrp]

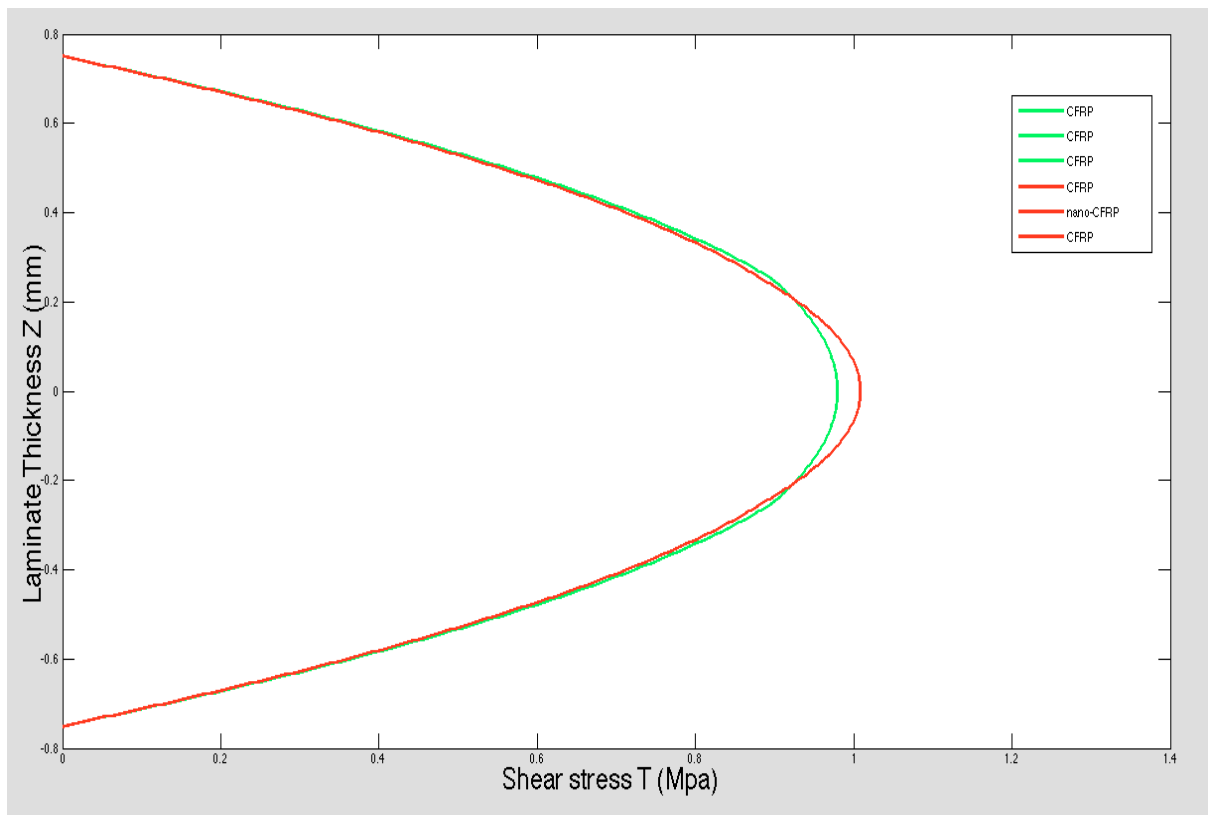


fig.30 T_{yz} Distribution of 45-0-45 [cfrp nano-cfrp cfrp]

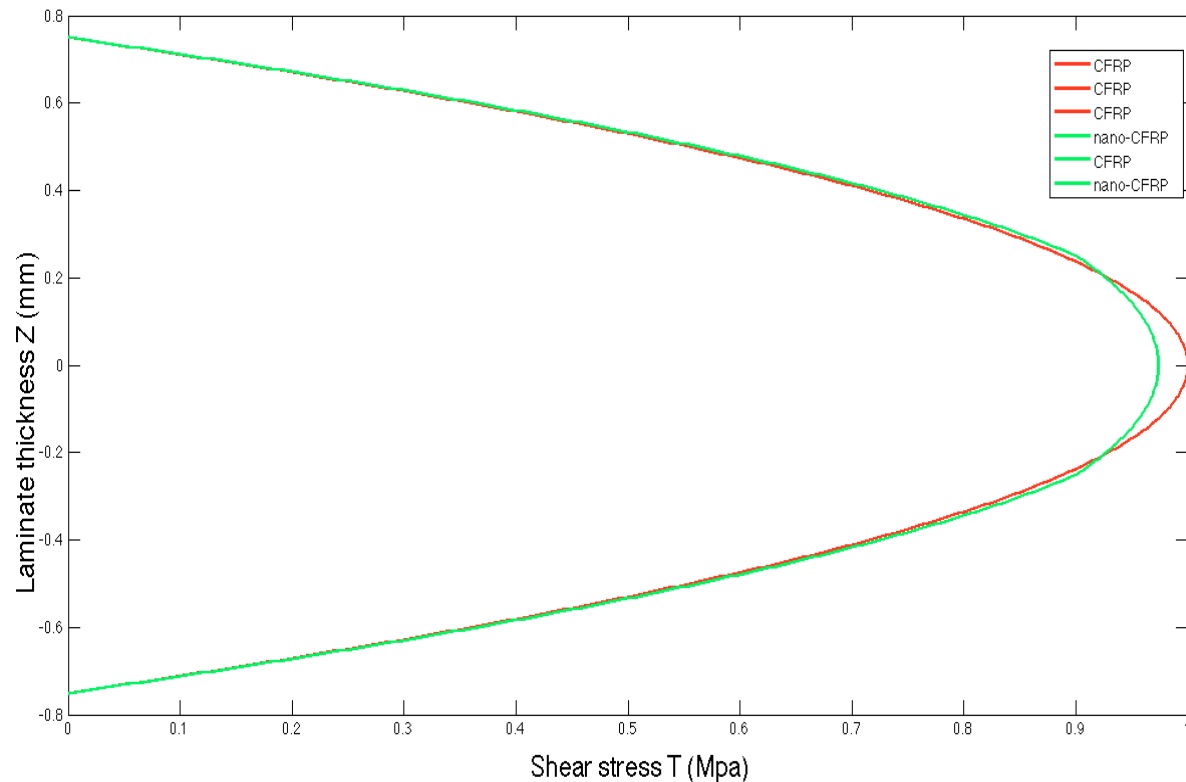


fig.31 T_{yz} Distribution of 0-0-0[nano-cfrp cfrp nano-cfrp]

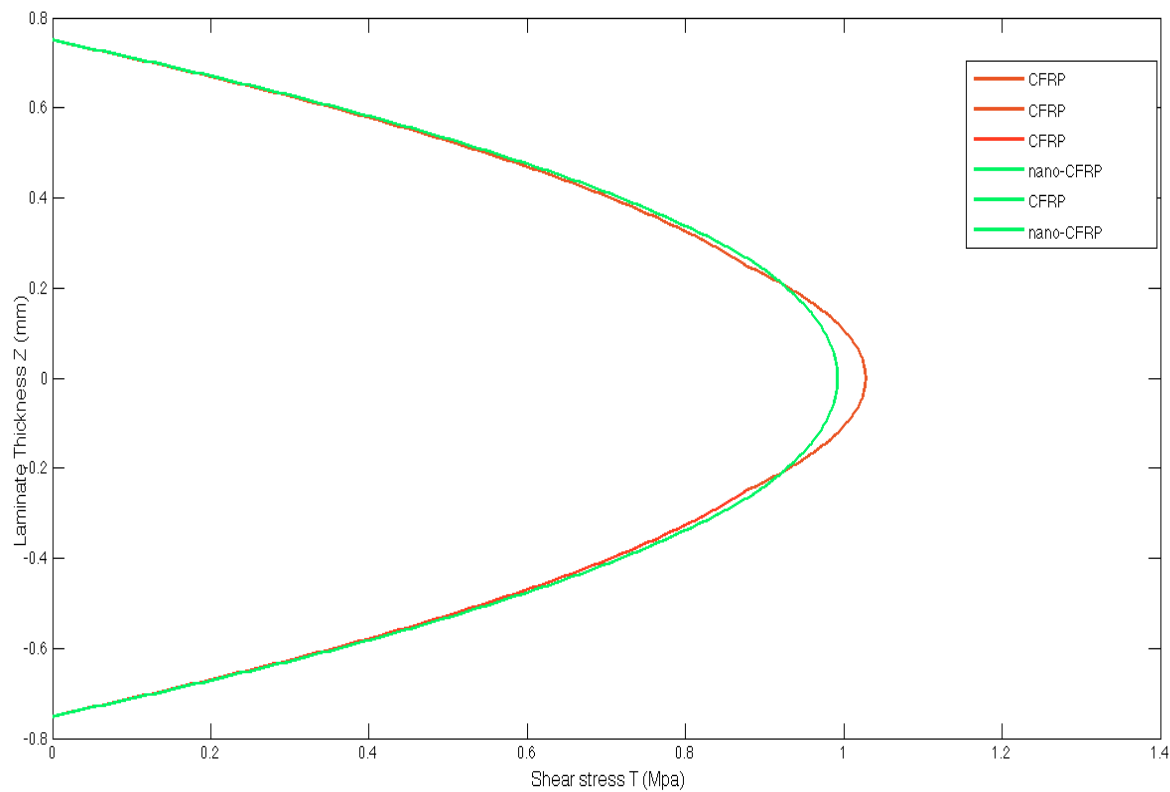


fig.32 T_{yz} Distribution of 0-45-0 [nano-cfrp cfrp nano-cfrp]

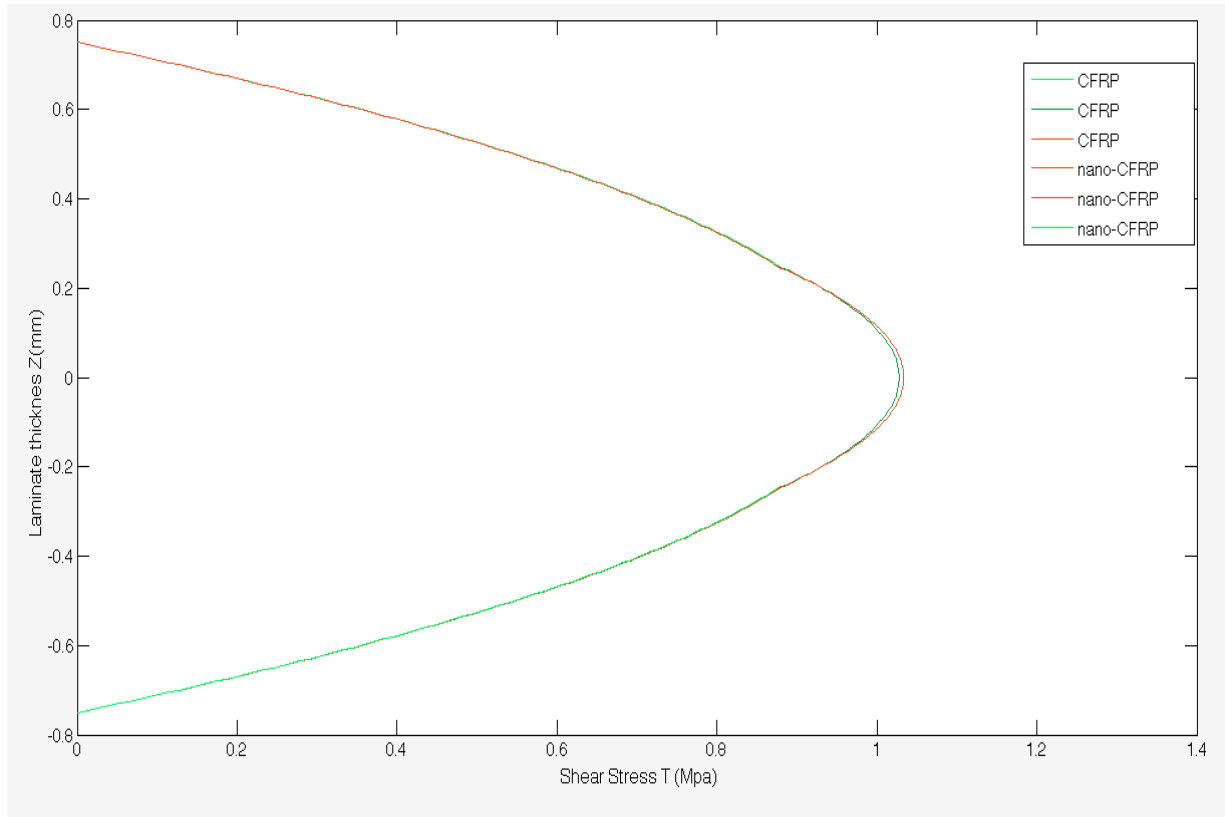


fig.33 T_{yz} Distribution of 0-45-0 [nano-cfrp nano-cfrp nano-cfrp]

orientation	Reference			Laminate : [cfrp,nano-cfrp,cfrp]		
	Max.lyr-1	Max.lyr-2	Max.lyr-3	Max.lyr-1	Max.lyr-2	Max.lyr-3
[0,0,0]	.8889	1	.8889	.8715 (-1.95)	1.0391 (3.91)	.8715 (-1.95)
[0,45,0]	.8766	1.0276	.8766	.8498 (-3.05)	1.0880 (5.87)	.8498 (-3.05)
[45,0,45]	.8980	.9795	.8980	.8851 (-1.43)	1.0086 (2.97)	.8851 (-1.43)
[0,90,0]	.5705	1.7165	.5705	.5676 (-.5)	1.7229 (0.37)	.5676 (-.5)

Table 5: Layer wise Maximum ILSS- T_{yz} values before and after nano inclusion of [cfrp,nano-cfrp,cfrp] system. % Difference is indicated in braces. Wt% of cnt =1 %

orientation	Reference			Laminate : [nano-cfrp,cfrp,nano-cfrp,]		
	Max.lyr-1	Max.lyr-2	Max.lyr-3	Max.lyr-1	Max.lyr-2	Max.lyr-3
[0,0,0]	.8889	1	.8889	.9006 (1.31)	.9737 (-2.63)	.9006 (1.31)
[0,45,0]	.8766	1.0276	.8766	.8923 (1.79)	.9923 (-3.43)	.8923 (1.79)
[45,0,45]	.8980	.9795	.8980	.9075 (.97)	.9587 (-2.12)	.9075 (.97)
[0,90,0]	.5705	1.7165	.5705	.6585 (1.71)	1.5183 (-11.54)	.6585 (1.71)

Table 6: Layer wise Maximum ILSS- T_{yz} values before and after nano inclusion of [nano-cfrp,cfrp,nano-cfrp,] system. % Difference is indicated in braces. Wt% of cnt =1 %

orientation	Reference			[nano-cfrp,nano-cfrp, nano-cfrp]		
	Max.lyr-1	Max.lyr-2	Max.lyr-3	Max.lyr-1	Max.lyr-2	Max.lyr-3
[0,0,0]	.8889	1	.8889	.8889 (0)	1 (0)	.8889 (0)
[0,45,0]	.8766	1.0276	.8766	.8741 (-.28)	1.0333 (.554)	.8741 (-.28)
[45,0,45]	.8980	.9795	.8980	.8893 (-.97)	.9765 (-.31)	.8893 (-.97)
[0,90,0]	.5705	1.7165	.5705	.6560 (14.98)	1.5239 (-11.22)	.6560 (14.98)

Table 7: Layer wise Maximum ILSS- T_{yz} values before and after nano inclusion of [nano-cfrp,nano-cfrp, nano-cfrp] system. % Difference is indicated in braces.

Wt% of cnt=1

orientation	Reference			Laminate : [cfrp,nano-cfrp,cfrp]		
	Max.lyr-1	Max.lyr-2	Max.lyr-3	Max.lyr-1	Max.lyr-2	Max.lyr-3
[0,0,0]	.8889	1	.8889	.8534 (-3.99)	1.0796 (7.96)	.8534 (-3.99)
[0,45,0]	.8766	1.0276	.8766	.8314 (-5.15)	1.1293 (9.89)	.8314 (-5.15)
[45,0,45]	.8980	.9795	.8980	.8715 (-2.95)	1.0391 (6.08)	.8715 (-2.95)
[0,90,0]	.5705	1.7165	.5705	.5633 (-1.26)	1.7324 (.92)	.5633 (-1.26)

Table 8: Layer wise Maximum ILSS- T_{yz} values before and after nano inclusion of [cfrp, nano-cfrp, cfrp] system. % Difference is indicated in braces.

Wt.% of cnt=2

orientation	Reference			Laminate : [nano-cfrp ,cfrp,nano-cfrp]		
	Max.lyr-1	Max.lyr-2	Max.lyr-3	Max.lyr-1	Max.lyr-2	Max.lyr-3
[0,0,0]	.8889	1	.8889	.90633 (1.96)	.9600 (-4)	.90633 (1.96)
[0,45,0]	.8766	1.0276	.8766	.9005 (2.72)	.9735 (-5.26)	.9005 (2.72)
[45,0,45]	.8980	.9795	.8980	.9108 (1.42)	.9505 (-2.96)	.9108 (1.42)
[0,90,0]	.5705	1.7165	.5705	.7146 (25.25)	1.392 (-18.90)	.7146 (25.25)

Table 9: Layer wise Maximum ILSS-T_{yz} values before and after nano inclusion of [nano-cfrp, cfrp, nano-cfrp] system. % Difference is indicated in braces.

Wt.% of cnt=2

orientation	Reference			[nano-cfrp , nano-cfrp,nano-cfrp]		
	Max.lyr-1	Max.lyr-2	Max.lyr-3	Max.lyr-1	Max.lyr-2	Max.lyr-3
[0,0,0]	.8889	1	.8889	.8889 (0)	1 (0)	.8889 (0)
[0,45,0]	.8766	1.0276	.8766	.8774 (.09)	1.0258 (-.17)	.8774 (.09)
[45,0,45]	.8980	.9795	.8980	.8975 (-.05)	.9804 (.09)	.8975 (-.05)
[0,90,0]	.5705	1.7165	.5705	.7049 (23.55)	1.403 (-18.26)	.7049 (23.55)

Table 10: Layer wise Maximum ILSS-T_{yz} values before and after nano inclusion of [nano-cfrp, nano-cfrp, nano-cfrp] system. % Difference is indicated in braces.

Wt.% of cnt=2

7.6 Conclusions

- From Tables 5-10
Its better to have same lamina orientation in all layers to have better load taking capability (shear load) when compared to laminates with different ply orientations.
- From Tables 7,10
when all layers are of cfrp or nano-cfrp or in short the youngs modulus E value is same for all layers ,the maximum value of ILSS obtained (.8889,1,.8889) are the upper limits of load the layers can handle. (given applied unit load).
- From Tables 7,10
Even when all the layers are reinforced with cnts, ILSS of all layers is not improved . Thus it can be concluded that there is no use of reinforcing all layers with cnts , rather focusing on Top ,bottom and middle layers individually according to requirement of design is optimal.
This can also be seen from the graphs where the curve gets smoothed when cnts are added and not all points lie outside the reference curve.
- From tables 5,6,9
Adding cnts to cfrp lamina brings significant increase in ILSS
 1. Unidirectional plies: 4% and 8% increase with 1% and 2% cnt addition
 2. Cross plies: upto 15% increase with 1% cnt and 25% increase with 2% addition respectively.

Conclusions

A novel micro mechanics model has been developed based on method of cells to predict the elastic modulus of nano-CFRP Hybrid composites. The method accounts for random orientation and agglomeration of nano-particles in the matrix and thus is very effective in predicting the composite elastic modulus, which is well accounted with available literature.

Extensive simulations have been carried out to study the effect of various reinforcement parameters such as orientation, aspect ratio, weight percentages and volume fraction of CFRP on the Elastic properties and expected results were obtained.

A gentle introduction has been given to the Laminate theory and effective mechanical properties of a Laminate system were predicted using Laminate theory. In addition to above the interlaminar shear stresses in laminates were calculated using a Simplified shear model and results were validated with literature. A Novel method was introduced to enhance the interlaminar shear stress without modifying the laminate parameters like thickness, number of layers and orientation of plies. Extensive simulations have been performed on proposed new method and objective results were displayed.

References

- [1] H. W. Kroto, J. R. Heath, S. C. O'Brien, R. F. Curl, R. E. Smalley, "C₆₀: Buckminsterfullerene", *Nature*, vol. 318, pp. 162-163, 1985.
- [2] O. Zhou, H. Shimoda, B. Gao, S. Oh, L. Fleming, G. Yue, "Material science of carbon nanotubes: fabrication, integration and properties of macroscopic structures of carbon nanotubes", *Accounts of Chemical Research*, vol. 35, pp. 1045-1053, 2002.
- [3] H. Dai, "Carbon nanotubes: synthesis, integration, and properties", *Accounts of Chemical Research*, vol. 35, pp. 1035-1044, 2002.
- [4] R. H. Baughman, A. A. Zakhidov, A. de Heer Walt, "Carbon nanotubes - the route toward applications", *Science*, vol. 297, no. 5582, pp. 787-792, 2002.
- [5] R. Saito, M. Fujita, G. Dresselhaus, M. S. Dresselhaus, "Electronic structure of chiral graphene tubules", *Applied Physics Letter*, vol. 60, no. 8, pp. 2204-2206, 1992.
- [6] S. Berber, Y-K. Kwon, and D. Tománek, "Unusually High Thermal Conductivity of Carbon Nanotubes", *Physical Review Letters*, vol. 84, no. 20, pp. 4613-4616, 2000.
- [7] M. J. Treacy, T. W. Ebbesen, and J. M. Gibson, "Exceptionally high Young's modulus observed for individual carbon nanotubes", *Nature*, vol. 381, pp. 678- 680, 1996.
- [8] S. B. Kharchenko, J. F. Douglas, J. Obrzut, E. A. Grulke, K. B. Migler, "Flow- induced properties of nanotube-filled polymer materials", *Nature Materials*, vol. 3, p.564-568, 2004.
- [9] N. H. Tai, M. K. Yeh, and J. H. Liu, "Enhancement of the mechanical properties of carbon nanotube/phenolic composites using a carbon nanotube network as the reinforcement", *Carbon*, vol. 42, pp. 774-777, 2004.
- [10] E. T. Thostenson, C. Li, and T.W. Chou, "Nanocomposites in Context", *Composite Science and Technology*, vol. 65, no. 3-4, pp. 491-516, 2005.
- [11] R. S. Ruoff, and D. C. Lorents, "Mechanical and thermal properties of carbon nanotubes", *Carbon*, vol. 33, pp. 925-930, 1995.
- [12] M-F. Yu, O. Lourie, M. J. Dyer, K. Moloni, T. F. Kelly, R. S. Ruoff, "Strength and breaking mechanism of multiwalled carbon nanotubes under tensile load", *Science*, vol. 287, pp. 637-640, 2000.
- [13] P. Calvert, "Nanotube composites: a recipe for strength", *Nature*, vol. 399, pp. 210-211, 1999.
- [14] T. S. Chow, "Mesoscopic Physics of Complex Materials", Springer-Verlag, New York Inc., 2000.
- [15] E. H. T. Teo, W. K. P. Yung, D. H. C. Chua, and B. K. Tay, "A carbon nanomattress: a new nanosystem with intrinsic, tunable, damping properties", *Advanced Materials*, no. 19, pp. 2941-2945, 2007.
- [16] I. Kang, Y. Y. Heung, J. H. Kim, J. W. Lee, R. Gollapudi, S. Subramaniam, S. Narasimhadhevara, D. Hurd, G. R. Kirikera, V. Shanov, M. J. Schulz, D. Shi, J. Boerio, S. Mall, and M. Ruggles-Wren, "Introduction to carbon nanotube and nanofiber smart materials", *Composites: Part B*, vol. 37, pp. 382-394, 2006.

- [17] R. H. Baughman, C. Cui, A. A. Zakhidov, Z. Iqbal, J. N. Barisci, and G. M. Spinks, "Carbo nanotube actuators", *Science*, vol. 284, no. 5418, pp. 1340- 1344, 1999
- [18] M. Tahhan, V. T. Truong, G. M. Spinks, G. G. Wallace, "Carbon nanotube and polyaniline composite actuators", *Smart Materials Structure*, vol. 12, pp. 626- 632, 2003.
- [19] E. Smela, "Conjugated polymer actuators for biomedical applications", *Advanced Materials*, vol. 15, no. 6, pp. 481-494, 2003.
- [20] J. R. Wood, H. D. Wagner, "Single-wall carbon nanotube as molecular pressure sensors" *Applied Physics Letter*, vol. 76, no. 20, pp. 2883-2885, pp. 2000.
- [21] J. Kong, N. R. Franklin, C. Zhou, M. G. Chapline, S. Peng, K. Cho, "Nanotube molecular wires as chemical sensors", *Science*, vol. 287, pp. 622-625, 2000.
- [22] S. Ghosh, A. K. Sood, N. Kumar, "Carbon nanotube flow sensors", *Science*, no. 200, no. 5609, pp. 1042-1044, 2003.
- [23] Y.J. Liu and X.L. Chen // *Mechanics of Materials* 69 (2003) 35.
- [24] X.L. Chen and Y.J. Liu // *Computational Materials Science* 29 (2004) 1.
- [25] Y. Liu, N. Nishimura and Y. Otani // *Computational Material Science*, in press.
- [26] K. Van Workum and J.J. de Pablo // *Nano Letters* 3 (2003) 1405.
- [27] S.A. Ospina, J. Restrepo and B.L. Lopez // *Materials Research Innovations* 7 (2003) 27.
- [28] N. Sheng, M.C. Boyce, D.M. Parks et al. // *Polymer* 45 (2004) 487.
- [29] T.M. Gates and J.A. Hinkley, NASA/TM-2003-212163.
- [30] G.M. Odegard, T.S. Gates, K.E. Wise, C. Park and E.J. Siochi // *Composites Science and Technology* 63 (2003) 1671.
- [31] Z. Hashin , *Journal of Applied Mechanics* 29 (1962) 143.
- [32] R. Hill , *Journal of the Mechanics and Physics of Solids* 12 (1964) 199.
- [33] R. Hill , *Journal of the Mechanics and Physics of Solids* 13 (1965) 213.
- [34] Z. Hashin and B.W. Rosen ,*Journal of Applied Mechanics* 31 (1964) 223.
- [35] J. Aboudi, *Mechanics of Composite Materials: a Unified Micromechanical Approach* (Elsevier, Amsterdam, 1991).
- [36] J.D. Eshelby ,*Proceedings of the Royal Society of London A* 241 (1957) 376.
- [37] B. Budiansky ,*Journal of the Mechanics and Physics of Solids* 13 (1965) 223.
- [38] T. Mori and K. Tanaka ,*Acta Metallurgica* 21 (1973) 571.
- [39] Y. Benveniste , *Mechanics of Materials* 6 (1987) 147.

- [40] J.C. Halpin and S.W. Tsai ,Environmental Factors in Composites Design, AFML-TR-67- 423.
- [41] R. Hill ,Journal of the Mechanics and Physics of Solids 11 (1963) 357.
- [42] R.J. Young, S.J. Eichhorn, Deformation mechanisms in polymer fibres and nanocomposites. Polymer, vol. 48, pp. 2–18, 2007.
- [43] T. Gómez-del Río, P. Poza, J. Rodríguez, M.C. García-Gutiérrez, J.J. Hernández, T.A. Ezquerra, Influence of single-walled carbon nanotubes on the effective elastic constants of poly (ethylene terephthalate). Compos. Sci. Technol, vol. 70, pp. 284–90, 2010.
- [44] S.K. Latifa, S. Chakraborty, Effective moduli of random short fiber composite: a probabilistic study. J. Reinf. Plast. Compos, vol. 23, pp. 751–60, 2004.
- [45] A. Montazeri, J. Javadpour, A. Khavandi, A. Tcharkhtchi, A. Mohajeri, Mechanical properties of multi-walled carbon nanotube/epoxy composites. Mater. Des, vol. 31, pp. 4202–8, 2010.
- [46] M.K. Yeh, N.H. Tai, Y.J. Lin, Mechanical properties of phenolic-based nanocomposites reinforced by multi-walled carbon nanotubes and carbon fibers. Compos Part A-Appl S, vol. 39, pp. 677–84, 2008
- [47] N. Sheng, M.C. Boyce, D.M. Parks, G.C. Rutledge, J.I. Abes, R.E. Cohen, Multiscale micromechanical modeling of polymer/clay nanocomposites and the effective clay particle. Polymer, vol. 45, pp. 487–506, 2004.
- [48] L. Liu, A.H. Barber, S. Nuriel, H.D. Wagner, Mechanical Properties of Functionalized Single-Walled Carbon-Nanotube/Poly (vinyl alcohol) Nanocomposites. Adv. Funct. Mater, vol. 15, pp. 975–80, 2005.
- [49] F. Dalmas, L. Chazeau, C. Gauthier, K. Masenelli-Varlot, R. Dendievel, J.Y. Cavaille, Multiwalled carbon nanotube/polymer nanocomposites: processing and properties. J. Polym. Sci., Part B: Polym. Phys, vol.; 43, pp. 1186–97, 2005
- [50] P.K. Valavala, G.M. Odegard, Modeling techniques for determination of mechanical properties of polymer, Rev.Adv.Mater.Sci, vol. 9, pp. 34-44, 2005.
- [51] J. Aboudi, The effective moduli of short-fiber composites. Int J Solids Struct, vol. 19, pp. 693–707, 1983.
- [52] Abhinav Alva and S Raja ,Dynamic characteristics of epoxy hybrid nanocomposite, journal of Reinforced Plastics and Composites November 2011 30: 1857-1867, doi:10.1177/0731684411429394.
- [53] Eslam Soliman1, Marwan Al-Haik2 and Mahmoud Reda Taha,On and off-axis tension behavior of fiber reinforced polymer composites incorporating multi-walled carbon nanotubes ,journal of Composite Materials 46(14) 1661–1675.
- [54] Myungsoo Kim, Young-Bin Park, Okenwa I. Okoli, Chuck Zhang, Processing, characterization, and modeling of carbon nanotube-reinforced multiscale composites, Composites Science and Technology 69 (2009) 335–342.

- [55] Mandar Kulkarni, David Carnahan, Kapil Kulkarni, Dong Qian, Jandro L. Abot ,Elastic response of a carbon nanotube fiber reinforced polymeric composite: A numerical and experimental study ,Composites: Part B 41 (2010) 414–421
- [56] Mao Sheng Chang, An investigation on the dynamic behavior and thermal properties of MWCNTs/FRP laminate composites, journal of Reinforced Plastics and Composites 29(24) 3593–3599.
- [57] R Rolfes and K.Rohwer , Improved Transverse shear stress in composite finite elements based on first order shear deformation theory, International journal for numerical methods in engineering vol. 40, 51—60 (1997)
- [58] Brett A Bednarcyk ,Jacob Aboudi , Determination of shear stress Distribution in a laminate from the Applied shear resultant-A simplified shear solution , NASA/CR—2007-215022
- [59] Florian H Gonjy, Malte H. g.Wichmann , Influence of different carbon nanotubes on mechanical properties of matrix composites-A comparative study , Composites Science and Technology 65 (2005) 2300–2313
- [60] Hiroaki Miyagawa ,Chiaki Sato , Transverse elastic Modulus of carbon fibers measured by Raman spectroscopy, Materials Science and Engineering A 412 (2005) 88–92.
- [61] Autar K. Kaw, Mechanics of Composite Materials Second Edition,ISBN 0-8493-1343-0.